Inorg. Chem. **1996,** *35,* 1101−1113

Synthesis, Structure, and Reactivity of Model Complexes of Copper Nitrite Reductase

Luigi Casella* and Oliviero Carugo

Dipartimento di Chimica Generale, Università di Pavia, Via Taramelli 12, 27100 Pavia, Italy

Michele Gullotti, Sergio Doldi, and Massimiliano Frassoni

Dipartimento di Chimica Inorganica, Metallorganica e Analitica, Università di Milano, Centro CNR,
Via Venezian 21, 20133 Milano, Italy

Received March 31, 1995⊗

The copper(I) and copper(II) complexes with the nitrogen donor ligands bis[(1-methylbenzimidazol-2-yl)methyl]amine (1-BB), bis[2-(1-methylbenzimidazol-2-yl)ethyl]amine (2-BB), *N*-acetyl-2-BB (AcBB), and tris[2-(1-methylbenzimidazol-2-yl)ethyl]nitromethane (TB) have been studied as models for copper nitrite reductase. The copper(II) complexes form adducts with nitrite and azide that have been isolated and characterized. The Cu(II)−(1-BB) and Cu(II)−AcBB complexes are basically four-coordinated with weak axial interaction by solvent or counterion molecules, whereas the Cu(II)−(2-BB) and Cu(II)−TB complexes prefer to assume five-coordinate structures. A series of solid state structures of Cu(II)−(1-BB) and −(2-BB) complexes have been determined. [Cu(1-BB)(DMSO-*O*)$_2$](ClO$_4$)$_2$: triclinic, $P\bar{1}$ (No. 2), $a = 9.400(1)$ Å, $b = 10.494(2)$ Å, $c = 16.760(2)$ Å, $\alpha = 96.67(1)°$, $\beta = 97.10(1)°$, $\gamma = 108.45(1)°$, V = 1534.8(5) Å^3, Z = 2, number of unique data [$I \geq 3\sigma(I)$] = 4438, number of refined parameters = 388, $R = 0.058$. [Cu(1-BB)(DMSO-*O*)$_2$](BF$_4$)$_2$: triclinic, $P\bar{1}$ (No. 2), $a = 9.304(5)$ Å, $b = 10.428(4)$ Å, $c = 16.834(8)$ Å, $\alpha = 96.85(3)°$, $\beta = 97.25(3)°$, $\gamma = 108.21(2)°$, V = 1517(1) Å^3, Z = 2, number of unique data [$I \geq 2\sigma(I)$] = 3388, number of refined parameters = 397, $R = 0.075$. [Cu(1-BB)(DMSO-*O*)(NO$_2$)](ClO$_4$): triclinic, $P\bar{1}$ (No. 2), $a = 7.533(2)$ Å, $b = 8.936(1)$ Å, $c = 19.168(2)$ Å, $\alpha = 97.66(1)°$, $\beta = 98.62(1)°$, $\gamma = 101.06(1)°$, V = 1234.4(7) Å^3, $Z = 2$, number of unique data [$I \geq 2\sigma(I)$] = 3426, number of refined parameters = 325, $R = 0.081$. [Cu(2-BB)(MeOH)(ClO$_4$)](ClO$_4$): triclinic, $P\bar{1}$ (No. 2), $a = 8.493(3)$ Å, $b = 10.846(7)$ Å, $c = 14.484(5)$ Å, $\alpha = 93.71(4)°$, $\beta = 103.13(3)°$, $\gamma = 100.61(4)°$, $V = 1270(1)$ Å^3, $Z = 2$, number of unique data [$I \geq 2\sigma(I)$] = 2612, number of refined parameters = 352, $R = 0.073$. [Cu(2-BB)(N$_3$)](ClO$_4$): monoclinic, $P2_1/n$ (No. 14), $a = 12.024(3)$ Å, $b = 12.588(5)$ Å, $c = 15.408(2)$ Å, $\beta = 101{,}90(2)°$, $V = 2282(1)$ Å^3, $Z = 4$, number of unique data [$I \geq 2\sigma(I)$] = 2620, number of refined parameters = 311, $R = 0.075$. [Cu(2-BB)(NO$_2$)](ClO$_4$)(MeCN): triclinic, $P\bar{1}$ (No. 2), $a = 7.402(2)$ Å, $b = 12.500(1)$ Å, $c = 14.660(2)$ Å, $\alpha = 68.14(1)°$, $\beta = 88.02(2)°$, $\gamma = 78.61(1)°$, $V = 1233.0(4)$ Å^3, $Z = 2$, number of unique data [$I \geq 2\sigma(I)$] = 2088, number of refined parameters = 319, $R = 0.070$. In all the complexes the 1-BB or 2-BB ligands coordinate the Cu(II) cations through their three donor atoms. The complexes with 2-BB appear to be more flexible than those with 1-BB. The nitrito ligand is bidentate in [Cu(2-BB)(NO$_2$)](ClO$_4$)(MeCN) and essentially monodentate in [Cu(1-BB)(DMSO-*O*)(NO$_2$)](ClO$_4$). The copper(I) complexes exhibit nitrite reductase activity and react rapidly with NO_2^- in the presence of stoichiometric amounts of acid to give NO and the corresponding copper(II) complexes. Under the same conditions the reactions between the copper(I) complexes and NO$^+$ yield the same amount of NO, indicating that protonation and dehydration of bound nitrite are faster than its reduction. The NO evolved from the solution was detected and quantitated as the [Fe(EDTA)(NO)] complex. The order of reactivity of the Cu(I) complexes in the nitrite reduction process is [Cu(2-BB)]$^+$ > [Cu(1-BB)]$^+$ > [Cu(TB)]$^+$ > [Cu(AcBB)]$^+$.

Introduction

The complex pattern of reactions undergone by inorganic nitrogen compounds in the environment is of vital importance for the ecological equilibrium on Earth.[1] In nitrogen fixation, dinitrogen is reduced to ammonia in a reaction catalyzed by a multimetal enzyme containing iron and molybdenum.[2] Dinitrogen is released into the atmosphere by the activity of a broad family of denitrifying bacteria found in soils and sediments.[3] These bacteria couple the anaerobic, stepwise reduction of oxidized nitrogen compounds to oxidative phosphorylation, in a respiratory chain analogous to the dioxygen consumption process occurring in aerobic organisms. All steps of biological denitrification depend on metal enzymes,[4] iron and copper enzymes being of particular importance. Nitrite reductases belonging to two different classes, containing heme cd_1 or copper as cofactor, are key enzymes in this process. The recent X-ray crystal structure determination of the copper nitrite

---

⊗ Abstract published in *Advance ACS Abstracts,* January 15, 1996.

[1] (a) *The Nitrogen and Sulphur Cycles*; Cole, J. A., Ferguson, S. J., Eds.; Cambridge University Press: Cambridge, U.K., 1988. (b) *Biology of Anaerobic Microorganisms*; Zehnder, A. B. J., Ed.; Wiley: New York, 1988. (c) Zumft, W. G. *The Prokaryotes*, 2nd ed.; Balows, A., et al., Eds.; Springer Verlag: Berlin, 1992; Vol. 1, p 554.

[2] (a) Kim, J.; Rees, D. C. *Science* **1992**, *257*, 1677. (b) Chan, M. K.; Kim, J.; Rees, D. C. *Science* **1993**, *260*, 792. (c) Kim, J.; Rees, D. C. *Biochemistry* **1994**, *33*, 389. (d) Eady, R. R.; Leigh, G. J. *J. Chem. Soc., Dalton Trans.* **1994**, 2739.

[3] (a) *Denitrification in Soil and Sediment*; Revsbech, N. B., Sørensen, J., Eds.; Plenum Press: New York, 1990. (b) Moody, A. D.; Ingledew, W. J. *Adv. Microbiol. Physiol.* **1990**, *31*, 225. (c) Hochstein, L. I.; Tomlinson, G. A. *Annu. Rev. Microbiol.* **1988**, *42*, 231.

[4] (a) Kroneck, P. M. H.; Zumft, W. G. In ref 3a, p 1. (b) Kroneck, P. M. H.; Beuerle, J.; Schumaker, W. *Met. Ions Biol. Syst.* **1992**, *28*, 455.

0020-1669/96/1335-1101$12.00/0

reductase from *Achromobacter cycloclastes* has shown that the functional unit contains one type 1 copper center and one type 2 copper center separated by 12.5 Å.[5] The role of the type 1 copper is to transfer an electron from reduced pseudoazurin to the type 2 copper,[6] which is the site of nitrite binding[7] and reduction.[8] Sequence identity and low-angle X-ray scattering measurements suggest that many other copper nitrite reductases conform to the same structural features.[9]

Chart 1

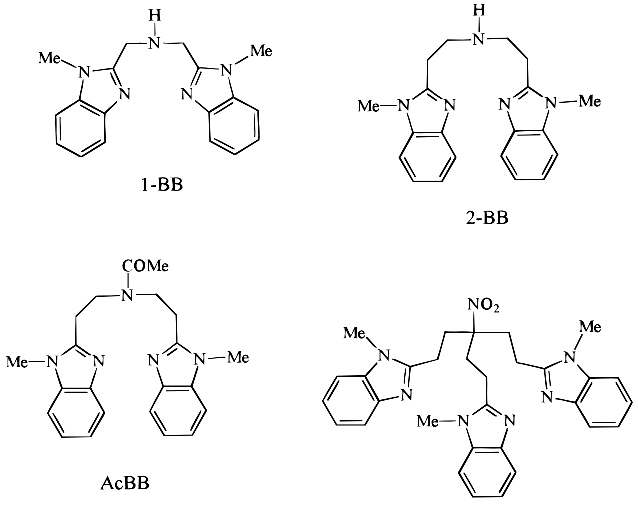

The economic and ecological importance of denitrification, with the prominent role played by copper enzymes in the transformation of N_xO_y species, and the number of studies in which the reaction between these species and other copper proteins, such as hemocyanin,[10] tyrosinase,[11] laccase,[12] ceruloplasmin,[13] ascorbate oxidase,[11] and cytochrome *c* oxidase,[14] is poorly understood have stimulated recent interest in the interaction of N_xO_y species with synthetic copper complexes. In particular, a few copper(II)−nitrite[15] and copper(I)−nitrite[16] adducts of potential relevance as models for the copper nitrite reductase−substrate complexes have been reported, as well as the reactions between mononuclear and dinuclear copper(I) complexes and NO[17,18] and the observation that on addition of acid the Cu(I)−NO_2^- adduct releases NO.[16b] In this paper we describe a series of copper(I) and copper(II) complexes with the nitrogen donor ligands reported in Chart 1 that allow some systematic investigation of the copper nitrite reductase biomimetic chemistry. In particular, we report the characterization of the adducts of the copper(II) complexes with nitrite and azide (an efficient inhibitor of the enzyme from *A. cycloclastes*),[20] including several X-ray structures, and the reactivity of the copper(I) complexes in the two steps of the nitrite reductase reaction, (1).

$$Cu^+{-}NO_2^- \xrightarrow{2H^+ \quad H_2O} Cu^+{-}NO^+ \longrightarrow Cu^{2+} + NO \qquad (1)$$

Results and Discussion

Synthesis. The attempt to mimic the tris(imidazole) array found in the type 2 copper center of *A. cycloclastes* requires the use of tridentate ligands with nitrogen donors. Those employed in the present investigation are a series of poly(benzimidazole) derivatives shown in Chart 1. The ligands 2-BB and TB were reported previously by us,[21,22] while 1-BB was obtained by reaction of iminodiacetic acid and *N*-methyl-*o*-diaminobenzene. The acetylated ligand AcBB[22] was used for comparison purposes, as a ligand with lower denticity, since *N*-acetylation prevents the central nitrogen atom of the chain from acting as a donor. The basic difference between 1-BB and 2-BB is the size of the chelate rings that they form upon coordination of a metal ion, which is smaller (five- *vs* six-membered) in the former case. We[23] and others[24] have already observed that this effect has an influence on the structure, spectra, and reactivity of copper complexes.

All the ligands readily form 1:1 complexes with copper(I) or copper(II). Those of copper(I) are air sensitive, especially in solution. The complexes $[Cu(1\text{-}BB)]^+$ and $[Cu[(2\text{-}BB)]^+$ are

---

(5) (a) Godden, J. W.; Turley, G.; Teller, D. C.; Adman, E. T.; Liu, M. Y.; Payne, W. J.; LeGall, J. *Science* **1991**, *153*, 438. (b) Adman, E. T.; Turley, S. K. In *Bioinorganic Chemistry of Copper*; Karlin, K. D., Tyeklár, Z., Eds.; Chapman & Hall: New York, 1993; p 397.

(6) (a) Kukimoto, M.; Nishiyama, M.; Murphy, M. E. P.; Turley, S.; Adman, E. T.; Horinouchi, S.; Beppu, T. *Biochemistry* **1994**, *33*, 5246. (b) Suzuki, S.; Kohzuma, T.; Deligeer; Yamauchi, K.; Nakamura, N.; Shidara, S.; Kobayashi, K.; Tagawa, S. *J. Am. Chem. Soc.* **1994**, *116*, 11145.

(7) (a) Howes, B. D.; Abraham, Z. H. L.; Lowe, D. J.; Brüser, T.; Eady, R. R.; Smith, B. E. *Biochemistry* **1994**, *33*, 3171. (b) Kohzuma, T.; Shidara, S.; Suzuki, S. *Bull. Chem. Soc. Jpn.* **1994**, *67*, 138.

(8) Libby, E.; Averill, B. A. *Biochem. Biophys. Res. Commun.* **1992**, *187*, 1529.

(9) (a) Fenderson, F.; Kumar, S.; Adman, E. T.; Liu, M. Y.; Payne, W. J.; LeGall, J. *Biochemistry* **1991**, *30*, 7180. (b) Glockner, A. B.; Jüngst, A.; Zumft, W. G. *Arch. Microbiol.* **1993**, *160*, 18. (c) Nishiyama, M.; Suzuki, J.; Kukimoto, M.; Ohnuki, T.; Horinouchi, S.; Beppu, T. *J. Gen. Microbiol.* **1993**, *139*, 725. (d) Ye, R. W.; Fries, M. R.; Bezborodniknov, S. G.; Averill, B. A.; Tiedje, J. M. *Appl. Environ. Microbiol.* **1993**, *59*, 250. (e) Grossman, J. G.; Abraham, Z. H. L.; Adman, E. T.; Neu, M.; Eady, R. R.; Smith, B. E.; Hasnain, S. S. *Biochemistry* **1993**, *32*, 7360.

(10) (a) Salvato, B.; Giacometti, G. M.; Beltramini, M.; Zilio, F.; Giacometti, G.; Magliozzo, R. S.; Peisach, J. *Biochemistry* **1989**, *28*, 680. (b) Westmoreland, T. D.; Wilcox, D. E.; Baldwin, M. J.; Mims, W. B.; Solomon, E. I. *J. Am. Chem. Soc.* **1989**, *111*, 6106.

(11) Gorren, A. C. F.; De Boer, E.; Wever, R. *Biochim. Biophys. Acta* **1987**, *916*, 38.

(12) Martin, C. T.; Morse, R. H.; Kanne, R. M.; Gray, H. B.; Malmström, B. G.; Chan, S. I. *Biochemistry* **1981**, *20*, 5147.

(13) Musci, G.; Di Marco, S.; Bonaccorsi di Patti, M. C.; Calabrese, L. *Biochemistry* **1991**, *30*, 9866.

(14) Brudvig, G. W.; Stevens, T. H.; Chan, S. I. *Biochemistry* **1980**, *19*, 5275.

(15) (a) Tolman, W. B. *Inorg. Chem.* **1991**, *30*, 4877. (b) Jiang, F.; Conry, R. R.; Bubacco, L.; Tyeklár, Z.; Jacobson, R. R.; Karlin, K. D.; Peisach, J. *J. Am. Chem.* Soc. **1993**, *115*, 2093. (c) Komeda, N.; Nagao, H.; Adachi, G.; Suzuki, M.; Uehara, A.; Tanaka, K. *Chem. Lett.* **1993**, 1521.

(16) (a) Halfen, J. A.; Mahapatra, S.; Olmstead, M. M.; Tolman, W. B. *J. Am. Chem. Soc.* **1994**, *116*, 2173. (b) Halfen, J. A.; Tolman, W. B. *J. Am. Chem. Soc.* **1994**, *116*, 5475.

(17) (a) Carrier, S. M.; Ruggiero, C. E.; Tolman, W. B. *J. Am. Chem. Soc.* **1992**, *114*, 4407. (b) Ruggiero, C. E.; Carrier, S. M.; Antholine, W. E.; Whittaker, J. W.; Cramer, C. J.; Tolman, W. B. *J. Am. Chem. Soc.* **1993**, *115*, 11285. (c) Ruggiero, C. E.; Carrier, S. M.; Tolman, W. B. *Angew. Chem., Int. Ed. Engl.* **1994**, *33*, 895.

(18) Paul, P. P.; Karlin, K. D. *J. Am. Chem. Soc.* **1991**, *113*, 6331.

(19) Paul, P. P.; Tyeklár, Z.; Farooq, A.; Karlin, K. D.; Liu, S.; Zubieta, J. *J. Am. Chem. Soc.* **1990**, *112*, 2430.

(20) Hulse, C. L.; Averill, B. A.; Tiedje, J. M. *J. Am. Chem. Soc.* **1989**, *111*, 2322.

(21) Casella, L.; Gullotti, M.; Radaelli, R.; Di Gennaro, P. *J. Chem. Soc., Chem. Commun.* **1991**, 1611.

(22) Casella, L.; Monzani, E.; Gullotti, M.; Gliubich, F.; De Gioia, L. *J. Chem. Soc., Dalton Trans.* **1994**, 3203.

(23) (a) Casella, L.; Gullotti, M.; Carugo, O.; Garofani, S.; Zanello, P. *Inorg. Chem.* **1993**, *32*, 2056. (b) Casella, L.; Gullotti, M. In *Bioinorganic Chemistry of Copper*; Karlin, K. D., Tyeklár, Z., Eds.; Chapman & Hall: New York, 1993; p 292.

(24) (a) Zubieta, J.; Karlin, K. D.; Hayes, J. C. In *Copper Coordination Chemistry*: *Biochemical and Inorganic Perspectives*; Karlin, K. D., Zubieta, J., Eds.; Adenine Press: Albany, NY, 1983; p 97. (b) Tyeklár, Z.; Jacobson, R. R.; Wei, N.; Murthy, N. N.; Zubieta, J.; Karlin, K. D. *J. Am. Chem. Soc.* **1993**, *115*, 2677.

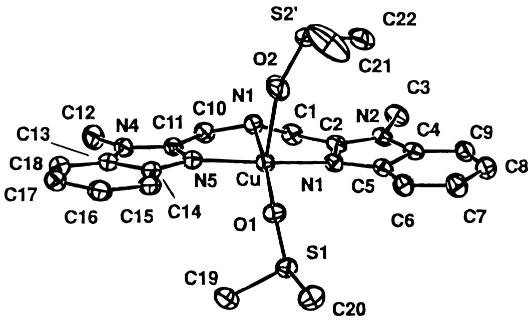

Figure 1. View of the $[Cu(1\text{-}BB)(DMSO\text{-}O)_2]^{2+}$ cation in the $[Cu(1\text{-}BB)(DMSO\text{-}O)_2](ClO_4)_2$ crystal (only S2′ is shown for clarity).

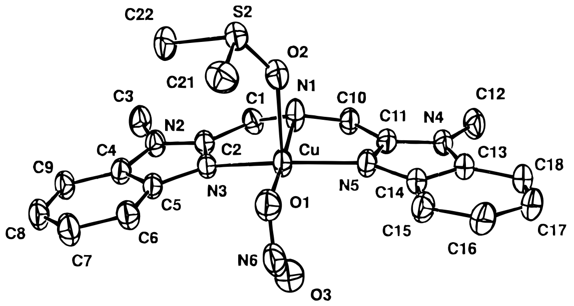

Figure 2. View of the $[Cu(1\text{-}BB)(DMSO\text{-}O)(NO_2)]^+$ cation in the $[Cu(1\text{-}BB)(DMSO\text{-}O)(NO_2)](ClO_4)$ crystal.

likely to be three-coordinate, with a T-shaped geometry similar to that found for bis(benzimidazole) thioether complexes.[25] The sharp ν(NH) bands occurring in their IR spectra at 3355 and 3310 cm^{-1}, respectively, red-shifted with respect to the free ligands, indicate that the central nitrogen donor is coordinated. The $[Cu(AcBB)]^+$ complex appears to be two-coordinate, since in this case the stretching frequency of the carbonyl group, which is the only potential donor group in the chain, shows no red shift with respect to the free ligand. The complex $[Cu(TB)]^+$ is also assumed to be three-coordinate, since in its ^{1}H NMR spectrum the signals of all methylene groups adjacent to the benzimidazole rings are downfield shifted to δ 4.1, removing the accidental degeneracy of the methylene signals of the free ligand at δ 3.8; also the shape of the aromatic signals is completely different for the complex. The structure may be either monomeric or dimeric, as found for the copper(I) complexes with tris(pyrazolyl)borate ligands.[26] The copper(II) complexes are coordinately unsaturated, and therefore, as shown by the crystal structures discussed below, they coordinate solvent molecules or counterions in the solid state and readily form adducts with exogenous anions.

Structures. (A) Complexes with 1-BB. Three copper(II) complexes with 1-BB have been structurally characterized: $[Cu(1\text{-}BB)(DMSO\text{-}O)_2](ClO_4)_2$ (Figure 1), $[Cu(1\text{-}BB)(DMSO\text{-}O)_2](BF_4)_2$ (Supporting Information), and $[Cu(1\text{-}BB)(DMSO\text{-}O)(NO_2)](ClO_4)$ (Figure 2). The first two complexes are five-coordinated in a distorted square pyramidal stereochemistry. $[Cu(1\text{-}BB)(DMSO\text{-}O)(NO_2)](ClO_4)$ may also be considered five-coordinated, since one of the oxygen atoms of the NO_2^- ligand is quite far from the metal [Cu−O3 = 2.671(8) Å].[27] Thus, also $[Cu(1\text{-}BB)(DMSO\text{-}O)(NO_2)](ClO_4)$ can be seen in a distorted square pyramidal stereochemistry. Therefore, the stereochemistry of these complexes can be described with a sulfoxide oxygen atom (O2) in the apical position and with the four basal positions occupied by the imidazole (N1 and N3) and amino (N5) nitrogen atoms of the 1-BB ligand and an oxygen atom (O1), which belongs to a sulfoxide ligand in the case of $[Cu(1\text{-}BB)(DMSO\text{-}O)_2](ClO_4)_2$ and $[Cu(1\text{-}BB)(DMSO\text{-}O)_2](BF_4)_2$ and to a nitrite ligand in the case of $[Cu(1\text{-}BB)(DMSO\text{-}O)(NO_2)](ClO_4)$.

$[Cu(1\text{-}BB)(DMSO\text{-}O)_2](ClO_4)_2$ and $[Cu(1\text{-}BB)(DMSO\text{-}O)_2](BF_4)_2$ are isomorphous and have been submitted to crystal structure analysis since they were obtained by different reactions (see below). In these two complexes, a sixth coordinative position, at the apex of a distorted octahedron, could be occupied by a monodentate perchlorate [Cu−O1] = 2.874(4) Å] or by a monodentate tetrafluoroborate [Cu−F = 2.849(5) Å]. However, both the high values of these bond distances and the fact that the same arrangement is shown by two quite different anions (ClO_4^- and BF_4^-) suggest that these metal−anion contacts should be better considered as due to electrostatic stabilization of the crystal packing.[28]

If the nitrite oxygen atom O3 is disregarded as a donor in $[Cu(1\text{-}BB)(DMSO\text{-}O)(NO_2)](ClO_4)$, the coordinative bond distances are very similar in all three complexes. The Cu−O1 one is slightly shorter when O1 belongs to the nitrite ligand [1.962(6) Å] than when it belongs to a sulfoxide [1.980(4) Å or 1.982(3) Å]. Other differences among the coordinative bond distances might be a consequence of different packing forces. Again disregarding the nitrite oxygen atom O3 in $[Cu(1\text{-}BB)(DMSO\text{-}O)(NO_2)](ClO_4)$, also the coordinative bond angles centered on the Cu^{2+} ion are very similar in all three complexes. The *trans*-basal ones range between 168.9(2) and 173.9(3)° [O1−Cu−O2] and between 157.6(2) and 161.8(2)° [N3−Cu−N5]. The *cis*-basal ones are near 90°, though those involving the two chelate rings are always smaller than the others. The apical−basal bond angles range between 83.0(2) and 101(2)°. Bond distances and angles within 1-BB ligands are very similar in all three complexes and fall in the expected range.[29] Also the geometries of the sulfoxide ligands are as expected.[30] This ligand frequently coordinates copper(II) through the oxygen atom, preferring this coordination mode to the S-coordination. The DMSO ligand in the apical position is disordered, as occurs quite often, with the sulfur atom statistically distributed on opposite sides of the plane defined by the O2, C21, and C22 atoms. The nitrite ligand chelates the Cu^{2+} ion very asymmetrically; the Cu−O3 bond [2.678(8) Å] is much longer than the Cu−O1 one [1.962(6) Å], and consequently also the N−O3 bond [1.20(1) Å] is much shorter than the N−O1 bond [1.25(1) Å].

(B) Complexes with 2-BB. Three copper(II) complexes with 2-BB have been characterized: $[Cu(2\text{-}BB)(MeOH)(ClO_4)]ClO_4$ (Figure 3), $[Cu(2\text{-}BB)(N_3)]ClO_4$ (Figure 4), and $[Cu(2\text{-}BB)(NO_2)]ClO_4\cdot MeCN$ (Figure 5). All of them are cationic, and in all cases the 2-BB ligand coordinates the copper(II) cation through its imidazole (N1 and N3) and amino (N5) nitrogen atoms. However, both the coordination numbers and stereochemistries of these three complexes are quite different.

In $[Cu(2\text{-}BB)(MeOH)(ClO_4)]ClO_4$, the metal center is five-coordinated in a compressed trigonal bipyramidal stereochemistry, with the two imidazole nitrogen atoms N1 and N3 in axial positions and the amino nitrogen atom N5, the perchlorate

---

(25) Dagdigian, J. V.; McKee, V.; Reed, C. A. *Inorg. Chem.* **1982**, *21*, 1332.

(26) (a) Mealli, C.; Arcus, C. S.; Wilkinson, J. L.; Marks, T. J.; Ibers, J. A. *J. Am. Chem. Soc.* **1976**, *98*, 711. (b) Carrier, S. M.; Ruggiero, C. E.; Houser, R. P.; Tolman, W. B. *Inorg. Chem.* **1993**, *32*, 4889.

(27) Hitchman, M. A.; Rowbottom, G. L. *Coord. Chem. Rev.* **1982**, *42*, 55.

(28) Rosenthal, M. R. *J. Chem. Educ.* **1973**, *50*, 331.

(29) Allen, F. H.; Kennard, O.; Watson, D. G.; Brammer, L.; Orpen, A. G. Taylor, R. *J. Chem. Soc., Perkin Trans. 2* **1987**, S1.

(30) Calligaris, M.; Carugo, O. *Coord. Chem. Rev.*, submitted for publication.

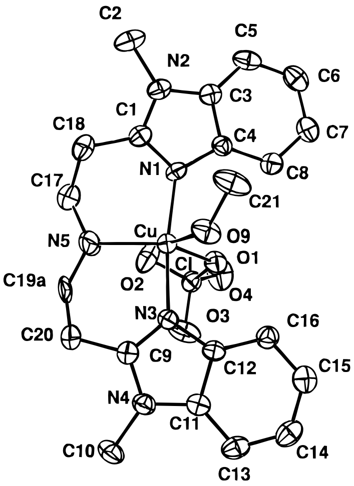

Figure 3. View of the $[Cu(2\text{-}BB)(MeOH)(ClO_4)]^+$ cation in the $[Cu(2\text{-}BB)(MeOH)(ClO_4)](ClO_4)$ crystal (only C19a is shown for clarity).

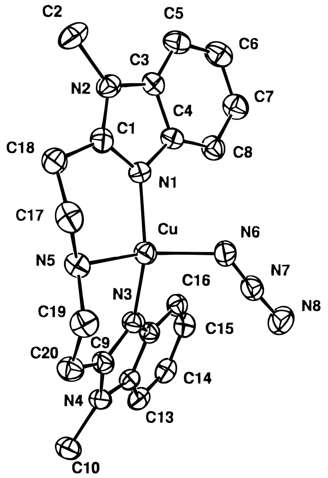

Figure 4. View of the $[Cu(2\text{-}BB)(N_3)]^+$ cation in the $[Cu(2\text{-}BB)(N_3)](ClO_4)$ crystal.

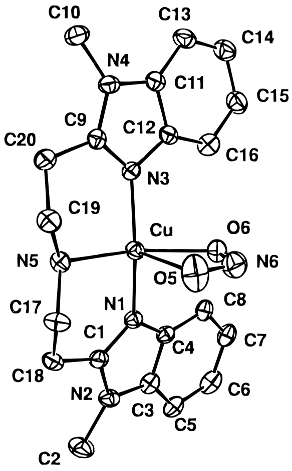

Figure 5. View of the $[Cu(2\text{-}BB)(NO_2)]^+$ cation in the $[Cu(2\text{-}BB)(NO_2)](ClO_4)(MeCN)$ crystal.

oxygen atom O1, and the methanol oxygen atom O9 in equatorial positions. In fact, the N1−Cu−N3 angle [171.6(3)°] approaches 180°, the equatorial bond angles centered on the Cu^{2+} ion range between 114.5(4) and 126.3(4)°, and the axial−equatorial bond angles range between 86.6(6) and 94.5(3)°.

In $[Cu(2\text{-}BB)(N_3)]ClO_4$, the metal center is four-coordinated in a stereochemistry intermediate between square planar and tetrahedral. In fact, the bond angles centered on the Cu^{2+} ion range between 91.1(3) and 150.5(3)°.

In $[Cu(2\text{-}BB)(NO_2)]ClO_4{\cdot}MeCN$, the stereochemistry of the metal center can be described as intermediate between those of the other two copper(II)/2-BB complexes, since the nitrite ligand chelates the Cu^{2+} ion, but with an obviously very small bite. So, although the coordination number is 5, as in $[Cu(2\text{-}BB)(MeOH)(ClO_4)]ClO_4$, the overall stereochemistry is more similar to that of the four-coordinated $[Cu(2\text{-}BB)(N_3)]ClO_4$ complex. In fact, the bond angles N1−Cu−N3, N1−Cu−N5, and N3−Cu−N5 have very close, although statistically different, values in $[Cu(2\text{-}BB)(NO_2)]ClO_4{\cdot}MeCN$ and $[Cu(2\text{-}BB)(N_3)]ClO_4$.

The above results indicate the quite high flexibility of the 2-BB ligand. In particular, it is worth noting that the N1−Cu−N3 angle can widen from 150.5(3)° in $[Cu(2\text{-}BB)(N_3)]ClO_4$ or 156.8(3)° in $[Cu(2\text{-}BB)(NO_2)]ClO_4{\cdot}MeCN$ to 171.6(3)° in $[Cu(2\text{-}BB)(MeOH)(ClO_4)]ClO_4$, without deforming the N1−Cu−N5 and N3−Cu−N5 angles, which have very similar values in all three complexes. It is also interesting to observe that the Cu−X (X = N1, N3, N5) bond distances are not seriously affected by the variation of stereochemistry at the metal center. All these coordinative bonds have statistically equal values and fall in the expected range.[31] Also the bond distances and angles of the 2-BB ligand do not feel the variation of stereochemistry at the metal center. The main statistically significant differences can be explained, at least in part, by the statistical disorder affecting carbon atom C19 in $[Cu(2\text{-}BB)(MeOH)(ClO_4)]ClO_4$. Anyway, all the 2-BB bond distances fall in the expected range.[29]

The geometries of the additional ligands (ClO_4^-, MeOH, N_3^-, and NO_2^-) are as expected. Perchlorate deviates little from a tetrahedral shape [O−Cl−O angles range between 107.8(5) and 111.2(5)°], but the Cl−O1 bond [1.453(7) Å] is significantly longer than the other Cl−O bonds [which range between 1.392(9) and 1.409(7) Å], presumably as a consequence of the coordination of O1 to the metal center.[32] Azide is nearly linear [N6−N7−N8 = 176.3(9)°], but the two N−N bonds are statistically equal [1.150(8) and 1.172(9) Å] in spite of the end-on coordination of N_3^-, which often causes small differences in the two bond lengths.[33] Both the methanol and azide molecules are bent by about 120° with respect to their ligands on copper(II). The chelation of the nitrite ligand is very asymmetric [Cu−O5 = 2.439(8) Å, Cu−O6 = 2.008(6) Å], with the consequent expected distortion of the NO_2^- ion from C_{2v} symmetry [N6−O5 = 1.23(1) Å, N6−O6 = 1.29(1) Å].[27]

(C) Comparison between 1-BB and 2-BB Structures. The two bis(benzimidazole) ligands 1-BB and 2-BB are closely similar, the only difference being in the alkyl chain between the secondary amino group and the heterocyclic moiety, which contains two carbon atoms in 2-BB and one carbon atom in 1-BB. Such a small difference does not cause important consequences when only intraligand bond distances and angles are considered but has important effects on the stereochemistry of coordination to the metal center. In the complexes with 1-BB only five-membered chelate rings can be formed, while only six-membered chelate rings can be formed in the case of 2-BB. Therefore, the geometry of the interaction between Cu^{2+} and the donor atoms is quite different in the two cases. The bond distances between the Cu^{2+} ion and the amino nitrogen atom are shorter in the case of 2-BB than in the case of 1-BB.

---

[31] Orpen, A. G.; Brammer, L.; Allen, F. H.; Kennard, O.; Watson, D. G.; Taylor, R. *J. Chem. Soc., Dalton Trans.* **1989**, S1.

[32] Gowda, N. M. N.; Naikar, S. B.; Reddy, G. K. N. *Adv. Inorg. Chem. Radiochem.* **1984**, *28*, 255.

[33] (a) Agnus, Y.; Louis, R.; Gisselbrecht, J.-P.; Weiss, R. *J. Am. Chem. Soc.* **1984**, *106*, 93. (b) Felthouse, T. R.; Hendrickson, D. N. *Inorg. Chem.* **1978**, *17*, 444. (c) Dori, Z.; Ziolo, R. F. *Chem. Rev.* **1973**, *73*, 249.

Moreover, the amino nitrogen atom is more tetrahedral in the case of 2-BB than in the case of 1-BB {the data for [Cu(2-BB)(MeOH)(ClO_4)]ClO_4 being disregarded because of the statistical disorder of atom C19}. The bond distances between the Cu^{2+} ion and the imidazole nitrogen atoms are not statistically different in 1-BB and 2-BB, but in the latter case the nitrogen lone pair can point directly at the metal cation, while in the case of 1-BB the Cu−N bond is bent of about 25° with respect to the nitrogen lone pair, though in both cases the cation lies on the imidazole plane. Moreover, the higher flexibility of a six-membered chelate ring with respect to a five-membered ring allows a higher relative mobility for the two benzimidazole moieties within the same ligand. The angles between the planes of the two benzimidazoles are much more restricted in the case of the 1-BB complexes, where they range between 7.1(7) and 12.6(3)°, than in the case of the 2-BB complexes, where they range between 13.9(6) and 38.1(2)°.

Another relevant consequence of the higher flexibility of the six-membered chelated rings with respect to the five-membered ones concerns the different steric requirements. Though the structures reported in the present paper could represent erratic examples, the [Cu(2-BB)]$^{2+}$ fragment seems to show a higher variability in expanding the metal coordination number: "true" coordination numbers 4 and 5 have been observed in the case of [Cu(2-BB)(N_3)]ClO_4 and [Cu(2-BB)(MeOH)(ClO_4)]ClO_4, respectively, together with a coordination number "intermediate" between 4 and 5 in the case of [Cu(2-BB)(NO_2)]ClO_4·MeCN. In contrast, the coordination numbers seem restricted to 5 in the case of the complexes with 1-BB, the only exception being [Cu(1-BB)(DMSO-*O*)(NO_2)](ClO_4), where a coordination number intermediate between 5 and 6 (but closer to 5, because of the basically monodentate character of the nitrito ligand) could be assigned. It seems also reasonable to suppose that the different steric requirements of the [Cu(2-BB)]$^{2+}$ and [Cu(1-BB)]$^{2+}$ fragments are one of the reasons that in the case of [Cu-(2-BB)(NO_2)]ClO_4·MeCN the nitrite anion is more symmetrically chelated to Cu^{2+} than in the case of [Cu(1-BB)(DMSO-*O*)(NO_2)](ClO_4).

Spectroscopy of Cu(II) Complexes. The difference in the mode of binding of nitrite to the [Cu(1-BB)]$^{2+}$ and [Cu(2-BB)]$^{2+}$ centers is reflected by the vibration modes of the anions in the adducts [Cu(1-BB)(NO_2)]ClO_4 and [Cu(2-BB)(NO_2)]ClO_4. In the former case the two $\nu(NO_2)$ stretchings are well separated, ν(N=O) at 1390 cm^{-1} and ν(N−O) buried under the broad and intense perchlorate band at 1100 cm^{-1}, while for the chelating nitro group of the second complex the two bands are closer in energy, $\nu_a(NO_2)$ occurring at 1334 cm^{-1} and $\nu_s(NO_2)$ at 1265 cm^{-1}, in agreement with expectation.[27,34a] The IR spectra of [Cu(TB)(NO_2)]ClO_4 and [Cu(AcBB)(NO_2)]ClO_4 suggest that a chelating nitro group is present also in these adducts. The $\nu_a(NO_2)$ mode occurs at 1383 cm^{-1} (shifted to 1360 cm^{-1} for the $^{15}NO_2^-$ adduct) in the former case and at 1360 cm^{-1} (1338 cm^{-1} for the $^{15}NO_2^-$ adduct) in the second case, while the ν_s-(NO_2) mode occurs at 1210 cm^{-1} (red-shifted to ~1200 and almost submerged under the broad perchlorate band for the $^{15}NO_2^-$ adduct) and 1245 cm^{-1} (1241 cm^{-1} in the $^{15}NO_2^-$ adduct), respectively. The main IR signature of coordinated azide is little sensitive to the mode of binding of the anion.[34] In the spectra of the present series of azide adducts, the $\nu_a(N_3)$ mode occurs in the range 2054−2110 cm^{-1}. Though it is almost coincident for [Cu(2-BB)(N_3)]ClO_4 and [Cu(AcBB)(N_3)]ClO_4, in the former complex the anion is monodentate, while in the latter it is probably bridging (and the complex binuclear), as suggested below by the electronic spectrum and the EPR behavior of the complex. The absence of a detectable $\nu_s(N_3)$ mode in the range ~1300 cm^{-1} for [Cu(AcBB)(N_3)]ClO_4 supports a dimeric formulation for this complex.

The electronic and EPR spectra of the copper(II) complexes and their nitrite and azide adducts show they have a tendency to assume a tetragonal field in solution. For most of the complexes derived from 1-BB and AcBB the presence of a single d−d band in the optical spectrum, between 630 and 670 nm (Table 1), indicates basically four coordinated species, with weak axial interaction. On the other hand, the d−d spectra of the complexes derived from 2-BB and TB generally display two bands, with a more intense high-energy component, which suggest square pyramidal structures.[35] According to this interpretation, the coordination mode of nitrite found in the structures of the adducts [Cu(1-BB)(NO_2)]$^+$ and [Cu(2-BB)-(NO_2)]$^+$ would seem to be maintained in solution, and we presume that nitrite acts as a chelating ligand also in [Cu(TB)-(NO_2)]$^+$ and [Cu(AcBB)(NO_2)]$^+$ (where the AcBB ligand is also bidentate). In the case of the azide adducts, according to the established trend[36] and as shown by the structure of [Cu-(2-BB)(N_3)]$^+$, since the charge of the copper(II) complexes is dipositive and one of the in-plane positions is accessible, coordination of the anion occurs equatorially. A solvent molecule completes the coordination set of five-coordinate complexes. The general trend in the d−d transitions suggests that the nitrite ligand lies lower in the spectrochemical series than azide in these copper(II) complexes.

The EPR data obtained from frozen solutions are consistent with the above conclusions, since the spectra show the characteristic pattern for tetragonal stereochemistries ($g_{\parallel} > g_{\perp}$) (Table 2). In several cases, the reduced values of the hyperfine constant $|A_{\parallel}|$ suggest some significant pseudotetrahedral distortion of the tetragonal chromophore. The azide adduct [Cu-(AcBB)(N_3)]$^+$ is completely EPR silent. This behavior was already noted for the copper(II)−hydroxo complex with the same ligand[22] and suggests the presence of binuclear, dibridged species in both cases, with strong antiferromagnetic coupling between the copper(II) centers.

Very important for the description of the spectroscopic properties of the complexes are the charge transfer bands occurring in the near-UV region (Table 1). Besides the intense intraligand absorptions below 300 nm, associated with benzimidazole $\pi \rightarrow \pi^*$ transitions, the spectra of the copper(II) complexes display a band near 350 nm and, for those derived from 1-BB and 2-BB, a detectable shoulder near 300 nm. These bands can be attributed to π(benzimidazole) → Cu(II)[23a,25] and σ(amino) → Cu(II)[37] LMCT transitions, respectively. However, the ~350-nm band increases remarkably in intensity in the series: [Cu(1-BB)]$^{2+}$ = [Cu(2-BB)]$^{2+}$ < [Cu(AcBB)]$^{2+}$ < [Cu-(TB)]$^{2+}$, with a change in extinction coefficient of 1 order of magnitude between the extremes. For [Cu(AcBB)]$^{2+}$ and [Cu-(TB)]$^{2+}$ this band is flanked by a shoulder at 310 nm that is missing in the spectra of their adducts with nitrite or azide. Addition of small amounts of hydroxide to solutions of the complexes shows that the more intense absorptions observed for [Cu(AcBB)]$^{2+}$ and [Cu(TB)]$^{2+}$ in the range 300−400 are

---

(34) (a) Nakamoto, K. *Infrared and Raman Spectra of Inorganic and Coordination Compounds*, 4th ed.; Wiley: New York, 1986; Part III. (b) Karlin, K. D.; Hayes, J. C.; Hutchinson, J. P.; Zubieta, J. *J. Chem. Soc., Chem. Commun*. **1983**, 376.

(35) (a) Hathaway, B. J. *Struct. Bonding* **1984**, *57*, 55. (b) Hathaway, B. J. In *Comprehensive Coordination Chemistry*; Wilkinson, G., Ed.; Pergamon: New York, 1987; Vol. 5, p 533.

(36) Casella, L.; Gullotti, M.; Pallanza, G.; Buga, M. *Inorg. Chem*. **1991**, *30*, 221.

(37) Lever, A. B. P. *Inorganic Electronic Spectroscopy*, 2nd ed.; Elsevier: Amsterdam, 1984; Chapter 5.

Table 1. Electronic Spectral Data for Copper(II) Complexes in MeCN Solution

complex	λ_{max}, nm (ϵ, M^{-1} cm^{-1})							
	intraligand			CT			d−d	
$[Cu(1\text{-}BB)]^{2+}$	244 (16 900)	272 (14 300)	280 (14 200)	300 sh (350)	350 (270)		636 (135)	
$[Cu(1\text{-}BB)(NO2)]^{+}$	246 (13 600)	272 (15 300)	280 (15 100)	300 sh (1400)	364 (1400)		630 (120)	
$[Cu(1\text{-}BB)(N_3)]^{+}$	244 (14 100)	272 (14 300)	280 (14 400)	300 sh (1500)	392 (2700)		622 (275)	730 sh (210)
$[Cu(2\text{-}BB)]^{2+}$	248 (16 300)	272 (13 300)	280 (11 700)	300 sh (650)	375 (260)		676 (190)	790 (170)
$[Cu(2\text{-}BB)(NO_2)]^{+}$	246 (14 300)	272 (15 000)	280 (11 500)	300 sh (700)	372 (450)		670 (210)	750 sh (170)
$[Cu(2\text{-}BB)(N_3)]^{+}$	246 (14 800)	272 (13 900)	280 (12 450)	300 sh (800)	420 (1800)		652 (500)	735 sh (450)
$[Cu(AcBB)]^{2+}$	250 (14 800)	274 (13 200)	280 (12 100)	310 sh (1000)	342 (800)		670 (45)	
$[Cu(AcBB)(NO_2)]$	250 (14 500)	272 (13 200)	280 (12 600)	374 (430)			674 (80)	
$[Cu(AcBB)(N_3)]^{+}$	252 (14 000)	272 (16 700)	282 (15 100)	370 sh (1500)	436 (1400)	500 sh (800)	656 (180)	
$[Cu(TB)]^{2+}$	252 (22 100)	274 (24 000)	280 (22 000)	310 sh (2200)	364 (2700)		710 (85)	870 (65)
$[Cu(TB)(NO_2)]^{+}$	254 (20 000)	276 (23 500)	280 (20 000)	370 (400)			645 (30)	870 (20)
$[Cu(TB)(N_3)]^{+}$	246 (22 300)	274 (25 000)	282 (22 500)	370 (2200)	440 (2130)		660 (280)	

Table 2. EPR Parameters of Copper(II) Complexes in Frozen MeCN Solutions at −150 °C

complex	$g_{\parallel}$	$g_{\perp}$	$10^{-4}\lvert A_{\parallel}\rvert$ (cm^{-1})
$[Cu(1\text{-}BB)]^{2+}$	2.273	2.060	170
$[Cu(1\text{-}BB)(NO_2)]^{+}$	2.261	2.065	173
$[Cu(1\text{-}BB)(N_3)]^{+}$ [a]	2.256	2.058	173
$[Cu(2\text{-}BB)]^{2+}$	*b*		
$[Cu(2\text{-}BB)(NO_2)]^{+}$	2.259	2.090	143
$[Cu(2\text{-}BB)(N_3)]^{+}$	2.259	2.089	139
$[Cu(AcBB)]^{2+}$	2.332	2.065	144
$[Cu(AcBB)(NO_2)]^{+}$	2.279	2.057	160
$[Cu(AcBB)(N_3)]^{+}$		(EPR silent)	
$[Cu(TB)]^{2+}$	2.335	2.078	148
$[Cu(TB)(NO_2)]^{+}$	2.296	2.064	170
$[Cu(TB)(N_3)]^{+}$	2.298	2.066	159

[a] In MeCN−MeOH. [b] Mixture of species.

Table 3. Nitrite Reductase Activity of Copper(I) Complexes at Room Temperature in MeCN Solution

system	reacn time (min)	% NO detected as [Fe(EDTA)(NO)]
$[Cu(1\text{-}BB)]^{+} + NO_2^{-} + 2H^{+}$	5	44
$[Cu(1\text{-}BB)]^{+} + NO^{+}$	5	47
$[Cu(2\text{-}BB)]^{+} + NO_2^{-} + 2H^{+}$	5	65
$[Cu(2\text{-}BB)]^{+} + NO^{+}$	5	66
$[Cu(2\text{-}BB)]^{+} + NO_2^{-}$	5	∼0
$[Cu(AcBB)]^{+} + NO_2^{-} + 2H^{+}$	5	25
$[Cu(AcBB)]^{+} + NO^{+}$	5	27
$[Cu(TB)]^{+} + NO_2^{-} + 2H^{+}$	5	31
$[Cu(TB)]^{+} + NO^{+}$	5	33
$[Cu(MeCN)_{4}]^{+} + NO_2^{-} + 2H^{+}$	5	15
$NO_2^{-} + 2H^{+}$	5	<5
$[Cu(2\text{-}BB)]^{2+} + NO_2^{-} + 2H^{+}$	15	<1
$[Cu(2\text{-}BB)(NO_2)]^{+} + 2H^{+}$	15	<1

in fact due to copper(II)−hydroxo complexes formed by the dissociation of bound water ($\Delta\epsilon \sim 2000$ M^{-1} cm^{-1} at [Cu(II)]:$[OH^-]$ = 1:1). This behavior was already noted for the previously reported $[Cu(TB)]^{2+}$ complex,[38] where the EPR-silent dimeric complex $[Cu(TB)(OH)]_2^{2+}$ is formed.

The azide complexes display the characteristic LMCT band near 400 nm. The position of this band correlates roughly with the effective charge on the Cu(II) center.[36] In the present series of complexes, we find that λ_{max} for the $\pi(N_3^-) \rightarrow$ Cu(II) LMCT transition increases in the order $[Cu(1\text{-}BB)(N_3)]^+ < [Cu(2\text{-}BB)(N_3)]^+ < [Cu(AcBB)(N_3)]^+ \sim [Cu(TB)(N_3)]^+$. This suggests that the ligand 1-BB has higher donor strength than 2-BB, in agreement with expectation (it forms five-membered rather than six-membered chelate rings) and the higher-energy position of the d−d bands of its complexes. On the basis of the above criterion, we would expect the AcBB complex to occupy the highest position in the series. However, the azide−Cu(II) LMCT band of this complex shows multicomponent structure, and together with the EPR silence of the adduct $[Cu(AcBB)(N_3)]^+$ (Table 2) discussed above, this indicates the compound is dimeric, with a double azide bridge.

Of greatest interest in the present context is the analysis of the near-UV region of the copper(II)−nitrite complexes, since very little is known about the optical properties of this chromophore. Free nitrite absorbs very weakly in the near-UV ($\lambda_{max} = 352$ nm, $\epsilon = 26$ M^{-1} cm^{-1} in methanol solution). The nitrite complexes reported here exhibit a band near 370 nm that is systematically more intense than that due to the benzimidazole to copper(II) LMCT (Table 1). As already noted, $[Cu(AcBB)]^{2+}$ and $[Cu(TB)]^{2+}$ are apparent exceptions because partial formation of the hydroxide complexes leads to abnormal increase of absorption in the same region. For the adducts $[Cu(2\text{-}BB)(NO_2)]^+$, $[Cu(AcBB)(NO_2)]^+$, and $[Cu(TB)(NO_2)]^+$, the intensities of the 370-nm band are very similar ($\epsilon = 400-450$ M^{-1} cm^{-1}) and suggest that an intensity contribution of about 200 M^{-1} cm^{-1} is due to the bound nitrite. Interestingly, for $[Cu(1\text{-}BB)(NO_2)]^+$ the intensity of this band is much higher ($\epsilon \sim 14\ 00$ M^{-1} cm^{-1}). We therefore propose that the origin of the 370-nm band is a copper(II)−nitrite charge transfer transition and that the intensity difference observed here for the two groups of nitrite adducts correlates with the mode of binding of the anion, *O*,*O*-bidentate chelate nitrite giving rise to weak absorption and *O*-monodentate nitrite to moderately intense absorption in the near-UV. Both the possibilities of $n(NO_2) \rightarrow d(Cu)$ LMCT and $d(Cu) \rightarrow \pi^*(NO_2)$ MLCT assignments apparently

---

(38) Alzuet, G.; Casella, L; Perotti, A.; Borras, J. *J. Chem. Soc., Dalton Trans.* **1994**, 2347.

Table 4. Crystal Data and Experimental Details for the Crystallographic Analyses of [Cu(2-BB)(MeOH)(ClO_4)](ClO_4) (**I**), [Cu(2-BB)(N_3)](ClO_4) (**II**), [Cu(2-BB)(NO_2)](ClO_4) (**III**), [Cu(1-BB)(DMSO-*O*)$_2$](ClO_4)$_2$ (**IV**), [Cu(1-BB)(DMSO-*O*)$_2$](BF_4)$_2$ (**V**), and [Cu(1-BB)(DMSO-*O*)(NO_2)](ClO_4) (**VI**)

	I	II	III	IV	V	VI
formula	$C_{21}H_{27}Cl_2CuN_5O_9$	$C_{20}H_{23}ClCuN_8O_4$	$C_{22}H_{26}ClCuN_7O_6$	$C_{22}H_{31}Cl_2CuN_5O_{10}S_2$	$C_{22}H_{31}B_2CuF_8N_5O_2S_2$	$C_{20}H_{28}ClCuN_6O_7S$
fw	627.92	538.45	583.49	724.09	698.80	592.54
system	triclinic	monoclinic	triclinic	triclinic	triclinic	triclinic
space group	$P\bar{1}$ (No. 2)	$P2_1/n$ (No. 14)	$P\bar{1}$ (No. 2)	$P\bar{1}$ (No. 2)	$P\bar{1}$ (No. 2)	$P\bar{1}$ (No. 2)
a (Å)	8.493(3)	12.024(3)	7.402(2)	9.400(1)	9.304(5)	7.533(2)
b (Å)	10.846(7)	12.588(5)	12.500(1)	10.494(2)	10.428(4)	8.936(1)
c (Å)	14.484(5)	15.408(2)	14.660(2)	16.760(2)	16.834(8)	19.168(2)
α (deg)	93.71(4)	90	68.14(1)	96.67(1)	96.85(3)	97.66(1)‘
β (deg)	103.13(3)	101.90(2)	88.02(2)	97.10(1)	97.25(3)	98.62(1)
γ (deg)	100.61(4)	90	78.61(1)	108.45(1)	108.21(2)	101.06(1)
Z	2	4	2	2	2	2
V (Å^3)	1270(1)	2282(1)	1233.0(4)	1534.8(5)	1517(1)	1234.4(7)
D_{calc} (Mg m^{-3})	1.643	1.567	1.572	1.567	1.530	1.602
cryst size (mm)	0.25 × 0.15 × 0.05	0.10 × 0.10 × 0.25	0.11 × 0.06 × 0.03	0.55 × 0.45 × 0.36	0.30 × 0.20 × 0.20	0.20 × 0.20 × 0.10
crystal descripn	plate	needle	plate	prism	prism	prism
no. of refl meas	4924	4777	4813	7215	7224	5513
no. of unique refl	4264	4126	4427	5482	5068	4272
no. of obs refl	2612	2620	2088	4438	3388	3426
criterion for obs	$I > 2\sigma(I)$	$I > 2\sigma(I)$	$I > 2\sigma(I)$	$I > 2\sigma(I)$	$I > 2\sigma(I)$	$I > 2\sigma(I)$
R_{int}	0.038	0.039	0.033	0.029	0.041	0.041
θ_{max} (deg)	70	70	70	70	70	70
h_{min},h_{max}	0,10	−1,14	0,9	−11,11	−11,11	−9,9
k_{min},k_{max}	−13,13	0,15	−15,15	−12,12	−12,12	−10,10
l_{min},l_{max}	−17,17	−18,18	−17,17	−3,20	−3,20	−3,23
R^a	0.073	0.075	0.070	0.058	0.075	0.081
$R_w{}^b$	0.053	0.074	0.073	0.060	0.076	0.111
GOF^c	1.144	1.725	1.462	1.358	2.134	1.790
no. of refined param	352	311	319	388	397	325

^{a} $R = \Sigma(|F_o| - |F_c|)/\Sigma|F_o|$. ^{b} $R_w = [\Sigma w(|F_o| - |F_c|)^2/\Sigma|F_o|^2]^{1/2}$. ^{c} $GOF = [\Sigma(|F_o| - |F_c|)^2/(N_o - N_v)]^{1/2}$.

exist for the near-UV band,[37] as discussed for the nitrite complexes of other metal ions.

Nitrite Reductase Reactivity. In the attempt to mimic the nitrite reduction process occurring at the type 2 center of the enzyme, some preliminary experiments were carried out by reacting the copper(I) complexes with $NaNO_2$ anaerobically. When diluted solutions of the reagents in methanol were used, a slow reaction occurred to produce green copper(II) species. In dry acetonitrile the reaction was very slow unless small amounts of acid were added. Under these conditions, a rapid evolution of NO took place. In order to prevent the occurrence of complex reactions between nitrogen oxide species and the Cu(I)/Cu(II) couple, we found it useful to apply a weak stream of inert gas to remove the NO produced in the reaction from contact with the solution. On passing the gas stream through a cool and anaerobic Fe(EDTA) solution, it was possible to detect and quantitate NO as the strong [Fe(EDTA)(NO)] complex.[39] Under the gas flow conditions employed, the recovery of NO is obviously lower than the theoretical amount; therefore, the yields of NO were determined relative to standard nitrite−ascorbate solutions. Some comparative data on the reactivity of the various copper(I) complexes in the nitrite reduction are reported in Table 3. Relatively short reaction times were considered because the prolonged flow of inert gas through the Fe(EDTA) solution led to a loss of [Fe(EDTA)(NO)] adduct. Thus, the order of reactivity found

$$[\mathrm{Cu(2\text{-}BB)}]^+ > [\mathrm{Cu(1\text{-}BB)}]^+ > [\mathrm{Cu(TB)}]^+ > [\mathrm{Cu(AcBB)}]^+$$

indicates relative rates rather than overall chemical conversions. Blank experiments showed that the amount of NO produced in the absence of the Cu(I) complexes was almost negligible, while some nitrite reductase activity was exhibited by [Cu(MeCN)$_4$]PF_6. Interestingly, by reacting the copper(I) complexes with $NO^+BF_4^-$ under the same conditions as with $NO_2^- + 2H^+$, the same amount of NO was detected in each case, indicating that protonation and dehydration of bound nitrite, according to the first step of reaction 1, must be faster than its reduction. As expected, neither the copper(II) complexes nor the preformed copper(II)−nitrite adducts are active in the nitrite reductase reaction, confirming the absence of nonspecific reactions in the copper(I) systems and strong binding of NO_2^- to the Cu(II) centers.

The Cu(II) species produced in the nitrite reductase reactions described above are the [Cu(ligand)]$^{2+}$ complexes. This was indicated by the UV−vis spectral properties of the final reaction solutions and confirmed by isolating the product of the reaction between [Cu(1-BB)]PF_6, $NaNO_2$, and HBF_4. The formulation of this product corresponded to [Cu(1-BB)](BF_4)(PF_6), which upon crystallization from a DMSO solution, deposited crystals of [Cu(1-BB)(DMSO-*O*)$_2$](BF_4)$_2$, whose structure was discussed in a previous section. We have tried to observe some reaction intermediates by following the reactions between either the Cu(I) species and $NO_2^- + 2H^+$ or between Cu(I) species and NO^+ at lower temperature (−20 to −40 °C) through EPR, after freezing the solutions in liquid nitrogen. In some instances, in the initial phase of the reaction it was possible to observe a weak and structured EPR signal (∼12 G), superimposed on more prominent Cu(II) signals, due to some intermediate species that we are currently trying to characterize. Several attempts were also made to isolate nitrite adducts of the copper(I) complexes, but we have been unable to obtain them in sufficiently pure form, even working at low temperature. The necessity to use nonprotic but polar solvents like acetonitrile to dissolve the Cu(I) complexes is a problem because the affinity of nitrite for the Cu(I) species is low and using an excess of nitrite salt inevitably leads to partial oxidation of the copper(I) species.

Conclusion. We have reported a series of complexes of potential interest in the context of copper nitrite reductase biomimetic chemistry. The copper(II) complexes form *O*-bonded nitrite adducts. This seems a common characteristic

---

(39) Fanning, J. C. *Coord. Chem. Rev.* **1991**, *110*, 235.

Table 5. Selected Positional Parameters and Their Estimated Standard Deviations for [Cu(1-BB)(DMSO-*O*)$_2$](ClO$_4$)$_2$

atom	*x*	*y*	*z*	B_{eq}[a] (Å^2)
Cu	−0.01479(8)	0.73649(7)	0.74846(4)	3.69(1)
S1	−0.2114(1)	0.5491(1)	0.84512(8)	4.19(3)
S2	−0.1192(3)	0.9631(3)	0.6141(2)	4.70(6)
S2′	−0.2240(4)	0.9045(3)	0.6602(2)	5.11(8)
O1	−0.2098(4)	0.6060(3)	0.7647(2)	4.23(8)
O2	−0.0950(5)	0.8409(4)	0.6497(3)	7.6(1)
N1	0.2059(4)	0.8565(4)	0.7474(3)	4.08(9)
N2	0.1386(5)	1.0932(4)	0.9023(3)	3.96(9)
N3	−0.0012(4)	0.8874(4)	0.8340(2)	3.66(9)
N4	0.2244(5)	0.5485(4)	0.6261(3)	4.6(1)
N5	0.0415(4)	0.6083(4)	0.6747(2)	3.88(9)
C1	0.2681(5)	0.9507(5)	0.8250(4)	4.5(1)
C2	0.1371(5)	0.9795(5)	0.8542(3)	3.8(1)
C3	0.2717(7)	1.2165(5)	0.9319(4)	5.6(2)
C4	−0.0088(5)	1.0745(5)	0.9135(3)	3.8(1)
C5	−0.0964(5)	0.9450(4)	0.8707(3)	3.6(1)
C6	−0.2530(6)	0.8944(5)	0.8682(3)	4.3(1)
C7	−0.3170(6)	0.9779(6)	0.9108(4)	5.1(1)
C8	−0.2291(6)	1.1062(5)	0.9531(4)	5.0(1)
C9	−0.0736(6)	1.1570(5)	0.9561(3)	4.7(1)
C10	0.2981(5)	0.7724(5)	0.7232(4)	4.6(1)
C11	0.1890(5)	0.6425(5)	0.6750(3)	4.0(1)
C12	0.3762(7)	0.5515(6)	0.6150(4)	6.4(2)
C13	0.0885(6)	0.4471(5)	0.5917(3)	4.4(1)
C14	=0.0266(6)	0.4840(5)	0.6220(3)	4.0(1)
C15	−0.1789(6)	0.4053(5)	0.5982(3)	4.5(1)
C16	−0.2097(7)	0.2886(6)	0.5406(3)	5.3(1)
C17	−0.0917(8)	0.2542(5)	0.5097(4)	5.7(2)
C18	0.0577(7)	0.3308(6)	0.5343(4)	5.6(1)
C19	−0.1742(7)	0.3942(6)	0.8234(4)	5.6(2)
C20	−0.4084(6)	0.4822(7)	0.8488(4)	6.1(2)
C21	−0.315(1)	0.914(1)	0.594(1)	17.6(5)
C22	−0.083(1)	1.0936(7)	0.6894(4)	8.7(2)

[a] $B_{eq} = (1/3)\sum_i\sum_j B_{ij}a_i^*a_j^*\mathbf{a}_i\cdot\mathbf{a}_j$.

Table 6. Selected Positional Parameters and Their Estimated Standard Deviations for [Cu(1-BB)(DMSO-*O*)$_2$](BF$_4$)$_2$

atom	*x*	*y*	*z*	B_{eq}[a] (Å^2)
Cu	0.9854(1)	0.2366(1)	0.24828(7)	4.11(3)
S1	0.7918(2)	0.0494(2)	0.3463(1)	4.77(5)
S2	0.7706(4)	0.4019(4)	0.1579(2)	6.2(1)
S2′	0.8827(6)	0.4620(5)	0.1149(3)	6.4(1)
O1	0.7910(5)	0.1058(5)	0.2664(3)	4.5(1)
O2	0.8970(2)	0.3331(5)	0.1495(3)	7.5(2)
N1	1.2053(6)	0.3540(6)	0.2453(4)	4.3(2)
N2	1.1421(7)	0.5954(5)	0.4012(4)	4.4(2)
N3	1.0026(6)	0.3895(5)	0.3334(3)	3.9(1)
N4	1.2253(7)	0.0453(6)	0.1258(4)	5.3(2)
N5	1.0419(6)	0.1068(5)	0.1752(3)	4.2(1)
C1	1.2693(9)	0.4513(7)	0.3225(5)	5.2(2)
C2	1.1412(8)	0.4825(7)	0.3534(4)	4.2(2)
C3	1.277(1)	0.7199(8)	0.4317(5)	6.6(3)
C4	0.9965(8)	0.5782(7)	0.4152(4)	4.1(2)
C5	0.9071(8)	0.4471(6)	0.3713(4)	3.8(2)
C6	0.7514(8)	0.3990(7)	0.3710(5)	4.8(2)
C7	0.6888(9)	0.4820(8)	0.4154(5)	5.8(2)
C8	0.780(1)	0.6117(8)	0.4578(5)	6.0(2)
C9	0.9334(9)	0.6608(7)	0.4581(5)	4.9(2)
C10	1.2997(9)	0.2711(8)	0.2223(5)	5.3(2)
C11	1.1890(8)	0.1385(7)	0.1745(4)	4.5(2)
C12	1.374(1)	0.0441(9)	0.1130(6)	7.4(3)
C13	1.0894(9)	−0.0549(7)	0.0915(4)	5.0(2)
C14	0.9711(9)	−0.0177(7)	0.1219(4)	4.6(2)
C15	0.8164(9)	−0.0986(7)	0.0977(4)	5.1(2)
C16	0.786(1)	−0.2145(8)	0.0394(5)	6.1(2)
C17	0.902(1)	−0.2495(8)	0.0075(5)	6.8(3)
C18	1.053(1)	−0.1729(8)	0.0325(5)	6.4(2)
C19	0.834(1)	−0.1034(8)	0.3239(6)	6.6(3)
C20	0.597(1)	−0.0208(9)	0.3506(6)	7.3(3)
C21	0.907(1)	0.5910(9)	0.1891(6)	9.9(3)
C22	0.685(1)	0.409(1)	0.077(1)	18.0(6)

[a] $B_{eq} = (1/3)\sum_i\sum_j B_{ij}a_i^*a_j^*\mathbf{a}_i\cdot\mathbf{a}_j$.

of copper(II) complexes with nitrogen donor ligands[15,17c] and is actually the mode in which the substrate binds to copper(II) in nitrite reductase.[7a] Whether the bidentate chelate or monodentate coordination type is adopted seems largely dictated by steric factors, the chelation mode being preferred in the absence of steric restrictions. Besides the IR technique, also the near-UV charge transfer band associated with the Cu(II)−NO$_2^-$ chromophore may be sensitive to the coordination type of the anion. The mode of nitrite binding to the copper(I) complexes with the same ligands may be different, though, and this problem remains unsolved at the moment. Tolman and co-workers found that on treatment of an excess of NO$_2^-$ with the copper(I) complex of a triazacyclononane ligand in methanol, a dimeric adduct containing a μ_2-(η^1-*N*:η^1-*O*) nitrite was formed,[16a] and this originated a mononuclear *N*-bonded Cu(I)−NO$_2^-$ adduct by treatment with PPh$_3$.[16b] The present copper(I) complexes are apparently much more reactive toward nitrite, and isolation of their adduct appears difficult. On the other hand, the data we currently have on the Cu(I)−NO$_2^-$ adduct and the copper(II) species formed in the initial phase of the Cu(I) + NO$_2^-$/2H$^+$ or Cu(I) + NO$^+$ reaction indicate they may not contain any *N*-bonded N$_x$O$_y$ residue.

The anaerobic reactions between the Cu(I) complexes reported here and NO$_2^-$ or NO$^+$ represent the first systematic study of the nitrite reductase reaction in model systems. While the activation of nitrite bound to Cu(I) on protonation was reported by Halfen and Tolman,[16b] we show here that protonation and dehydration of bound nitrite occur faster than its reduction. Although the existence of an intermediate Cu(I)−NO$^+$ species in the enzymatic reaction has never been directly proved, there is mechanistic evidence for its formation from the *in vitro* reactivity of the enzyme.[20,40] From the data in Table 3 it is evident that the increase in the number of donor groups in the ligand enhances the activity of the Cu(I) complex in the reaction, in spite of the lower accessibility of the Cu(I) center to NO$_2^-$ or NO$^+$. It is also clear that the increase of donor strength of the nitrogen donors (1-BB or 2-BB *vs* TB) facilitates electron transfer from Cu(I) to the bound NO$^+$ residue. In all these regards, the tris(imidazole) donor set for the type 2 Cu site of the enzyme represents an optimal arrangement. The higher reactivity of [Cu(2-BB)]$^+$ with respect to [Cu(1-BB)]$^+$ must be attributed to the higher flexibility of the ligand, a requisite that is certainly important to accommodate the strucutral changes involved in the complex upon the Cu(I) → Cu(II) redox change.

Experimental Section

All reagents from commercial sources were of the highest purity available and were used as received. Acetonitrile for spectroscopic and reactivity measurements was successively distilled from potassium permanganate, sodium carbonate, and calcium hydride. The ligands bis[2-(1-methylbenzimidazol-2-yl)ethyl]amine (2-BB), *N*-acetyl-2-BB (AcBB), and tris[2-(1-methylbenzimidazol-2-yl)ethyl]nitromethane (TB) were prepared as described previously.[21,22] [Cu(MeCN)$_4$]PF$_6$ was prepared by a literature method,[41] while the copper(II) complex [Cu(TB)][ClO$_4$]$_2$ was also reported recently by us.[38] The synthesis and manipulation of the copper(I) complexes were performed with Schlenk techniques. Elemental analyses were obtained at the microanalytical laboratory of the Chemistry Department in Milan. Infrared spectra were recorded on a Jasco FT-IR-5000 instrument. NMR spectra were recorded on Bruker WP-80 and AC-200 spectrometers, operating at

---

(40) (a) Ye, R. W.; Toro-Suarez, J.; Tiedje, J. M.; Averill, B. A. *J. Biol. Chem.* **1991**, *266*, 12848. (b) Jackson, M. A.; Tiedje, J. M.; Averill, B. A. *FEBS Lett.* **1991**, *291*, 41.

(41) Kubas, G. J. *Inorg. Synth.* **1979**, *19*, 90.

Table 7. Selected Positional Parameters and Their Estimated Standard Deviations for [Cu(1-BB)(DMSO-*O*)(NO_2)](ClO_4)

atom	x	y	z	B_{eq}[a] (Å^2)
Cu	0.1619(2)	0.2481(1)	0.30372(5)	5.15(2)
S2	−0.3244(3)	0.1366(2)	0.24154(9)	5.99(4)
O1	0.1222(8)	0.0381(6)	0.3267(3)	7.1(2)
O2	−0.1463(7)	0.2361(6)	0.2839(3)	6.8(1)
O3	0.4103(9)	0.0971(9)	0.3572(3)	9.7(2)
N1	0.173(1)	0.4643(7)	0.2775(3)	6.5(2)
N2	0.2435(9)	0.2864(6)	0.1033(3)	5.4(1)
N3	0.1974(8)	0.1998(6)	0.2041(2)	4.6(1)
N4	0.2706(9)	0.6003(7)	0.4712(3)	5.8(1)
N5	0.1988(8)	0.3675(6)	0.4014(3)	5.3(1)
N6	0.270(1)	0.0026(8)	0.3503(3)	8.4(2)
C1	0.247(1)	0.4808(8)	0.2125(4)	5.5(2)
C2	0.227(1)	0.3215(8)	0.1723(3)	4.9(2)
C3	0.270(1)	0.3917(9)	0.0517(4)	7.1(2)
C4	0.228(1)	0.1277(8)	0.0895(3)	5.2(2)
C5	0.198(1)	0.0739(8)	0.1526(3)	4.9(2)
C6	0.171(1)	−0.0815(8)	0.1556(4)	5.9(2)
C7	0.181(1)	−0.1795(9)	0.0940(4)	7.2(2)
C8	0.218(1)	−0.1217(9)	0.0319(4)	6.8(2)
C9	0.239(1)	0.0305(9)	0.0275(3)	6.2(2)
C10	0.258(1)	0.5890(8)	0.3380(3)	5.7(2)
C11	0.239(1)	0.5172(8)	0.4038(3)	5.2(2)
C12	0.319(1)	0.7664(9)	0.4924(4)	7.5(2)
C13	0.242(1)	0.4899(9)	0.5154(3)	5.7(2)
C14	0.201(1)	0.3452(8)	0.4725(3)	5.4(2)
C15	0.163(1)	0.2137(9)	0.5005(3)	6.2(2)
C16	0.166(1)	0.229(1)	0.5735(4)	7.5(2)
C17	0.212(1)	0.373(1)	0.6164(4)	7.5(2)
C18	0.250(1)	0.504(1)	0.5899(4)	7.2(2)
C21	−0.338(1)	−0.050(1)	0.2643(5)	7.6(2)
C22	−0.291(1)	0.090(1)	0.1533(4)	7.8(2)

[a] $B_{eq} = (1/3)\sum_i\sum_j B_{ij}a_i^*a_j^*\mathbf{a}_i\cdot\mathbf{a}_j$.

Table 8. Selected Positional Parameters and Their Estimated Standard Deviations for [Cu(2-BB)(MeOH)(ClO_4)](ClO_4)

atom	x	y	z	B_{eq}[a] (Å^2)
Cu	0.6619(1)	0.2410(1)	0.24292(9)	4.24(3)
Cl1	0.8156(3)	0.1520(2)	0.0650(2)	4.94(5)
O1	0.8402(7)	0.2525(6)	0.1413(5)	5.9(2)
O2	0.6442(8)	0.1122(9)	0.0260(6)	9.2(3)
O3	0.882(1)	0.0525(7)	0.1044(6)	9.4(3)
O4	0.896(1)	0.1961(9)	−0.0038(5)	9.3(2)
O9	0.7341(8)	0.3588(6)	0.3729(4)	6.0(2)
N1	0.5674(7)	0.3709(6)	0.1758(5)	4.2(2)
N2	0.3818(8)	0.4815(7)	0.1209(5)	5.0(2)
N3	0.7881(8)	0.1254(6)	0.3097(5)	4.2(2)
N4	0.8625(9)	−0.0532(6)	0.3477(5)	4.9(2)
N5	0.454(1)	0.1062(8)	0.1981(8)	9.4(3)
C1	0.410(1)	0.3725(8)	0.1538(6)	4.7(2)
C2	0.220(1)	0.518(1)	0.0927(8)	7.0(3)
C3	0.530(1)	0.5552(8)	0.1203(6)	4.5(2)
C4	0.649(1)	0.4872(8)	0.1569(6)	4.2(2)
C5	0.572(1)	0.6748(9)	0.0938(7)	5.9(3)
C6	0.738(1)	0.7228(9)	0.1032(7)	6.4(3)
C7	0.859(1)	0.6550(9)	0.1409(7)	5.8(3)
C8	0.816(1)	0.5370(8)	0.1670(6)	4.9(2)
C9	0.736(1)	0.0024(8)	0.3106(6)	4.4(2)
C10	0.854(1)	−0.1870(8)	0.3613(8)	6.4(3)
C11	1.004(1)	0.0384(8)	0.3730(6)	4.5(2)
C12	0.957(1)	0.1520(8)	0.3495(6)	4.4(2)
C13	1.168(1)	0.0323(9)	0.4155(7)	5.7(2)
C14	0.280(1)	0.144(1)	0.4317(7)	6.2(3)
C15	1.233(1)	0.2561(9)	0.4068(7)	5.8(3)
C16	1.072(1)	0.2631(8)	0.3666(6)	4.8(2)
C17	0.316(1)	0.139(1)	0.1323(9)	7.2(3)
C18	0.277(1)	0.263(1)	0.1599(7)	6.2(3)
C19a	0.465(2)	−0.020(2)	0.200(1)	6.0(5)
C19b	0.425(2)	0.004(2)	0.243(2)	8.0(6)
C20	0.560(1)	−0.0692(9)	0.2766(8)	6.2(3)
C21	0.719(2)	0.485(1)	0.3951(8)	8.2(3)

[a] $B_{eq} = (1/3)\sum_i\sum_j B_{ij}a_i^*a_j^*\mathbf{a}_i\cdot\mathbf{a}_j$.

Table 9. Selected Positional Parameters and Their Estimated Standard Deviations for [Cu(2-BB)(N_3)](ClO_4)

atom	x	y	z	B_{eq}[a] (Å^2)
Cu	0.08555(9)	0.9681(1)	0.83920(7)	4.72(2)
N1	0.1042(5)	0.8847(5)	0.9488(4)	4.5(1)
N2	0.1715(5)	0.8308(6)	1.0861(4)	5.1(2)
N3	0.1106(5)	0.9874(5)	0.7185(4)	4.8(1)
N4	0.1783(5)	1.0500(5)	0.6066(4)	4.9(1)
N5	0.2097(5)	1.0716(5)	0.8869(4)	4.9(1)
N6	−0.0790(5)	0.9527(7)	0.8110(4)	6.5(2)
N7	−0.1369(5)	0.9596(6)	0.7418(4)	5.5(2)
N8	−0.2005(6)	0.9640(8)	0.6732(5)	7.9(2)
C1	0.1781(6)	0.9054(7)	1.0244(5)	4.9(2)
C2	0.2415(8)	0.8232(9)	1.1769(6)	7.2(3)
C3	0.0878(6)	0.7593(7)	1.0512(5)	4.8(2)
C4	0.0446(6)	0.7953(6)	0.9637(5)	4.7(2)
C5	0.0451(7)	0.6749(7)	1.0874(5)	5.9(2)
C6	−0.0412(8)	0.6180(8)	1.0339(6)	6.8(2)
C7	−0.0824(8)	0.6495(7)	0.9446(6)	6.3(2)
C8	−0.0392(7)	0.7362(7)	0.9094(6)	5.6(2)
C9	0.1665(6)	1.0664(6)	0.6914(5)	4.7(2)
C10	0.2405(7)	1.1182(8)	0.5558(6)	6.2(2)
C11	0.1265(6)	0.9537(6)	0.5788(5)	4.7(2)
C12	0.0851(6)	0.9124(6)	0.6491(5)	4.5(2)
C13	0.1137(7)	0.8976(7)	0.4979(5)	5.5(2)
C14	0.0594(7)	0.8029(8)	0.4935(6)	6.2(2)
C15	0.0181(7)	0.7597(8)	0.5653(6)	6.0(2)
C16	0.0318(7)	0.8171(7)	0.6449(5)	5.2(2)
C17	0.2164(7)	1.0937(7)	0.9832(6)	6.2(2)
C18	0.2591(7)	0.9962(7)	1.0388(5)	5.8(2)
C19	0.1831(8)	1.1700(7)	0.8330(6)	5.8(2)
C20	0.2178(7)	1.1588(7)	0.7436(6)	5.7(2)

[a] $B_{eq} = (1/3)\sum_i\sum_j B_{ij}a_i^*a_j^*\mathbf{a}_i\cdot\mathbf{a}_j$.

80 and 200 MHz, respectively. Optical spectra were obtained on a HP 8452A diode array spectrophotometer. EPR spectra were measured in frozen solutions using a Varian E-109 spectrometer operating at X-band frequencies.

Bis[(1-methylbenzimidazol-2-yl)methyl]amine Dihydrate (1-BB·2H_2O). A mixture of iminodiacetic acid (22.5 mmol), *N*-methyl-*o*-phenylenediamine (45 mmol), and 6 M HCl (80 mL) was refluxed for 3 d. After cooling, concentration to a small volume of the solution under vacuum and cooling in ice yielded a precipitate of the hydrochloride salt of the product. This was collected by filtration. Upon addition of acetone to the filtrate, further material precipitated. The unified mixture of crude hydrochloride salts was dissolved in the minimum amount of warm water, and the solution was treated with excess dilute ammonia under stirring. The free base thus precipitated was filtered off, washed with small amounts of cold water, and dried under vacuum (yield 60%). Anal. Calcd for $C_{18}H_{23}N_5O_2$: C, 63.32; H, 6.79; N, 20.51. Found: C, 63.13; H, 6.99; N, 20.49. IR (Nujol, cm^{-1}): 3385 br, 3054 w, 1622 m, 1526 m, 1483 s, 1400 m, 1315 s, 1284 s, 1238 m, 1149 w, 1118 m, 1009 m, 930 w, 917 w, 878 w. NMR ($CDCl_3$): δ 2,08 (s, NH + H_2O), 3.77 (s, 6H, N − CH_3), 4.17 (s, 4H, CH_2), 7.2−7.4 and 7.7−7.8 (m, 8H, benzimidazole C−H).

Copper(I) Complexes. The synthesis of the copper(I) complexes was performed under argon as follows. To a solution of the ligand (1 mmol) in 40 mL of degassed ethanol (1-BB), dichloromethane−ethanol (2-BB), or dichloromethane (AcBB and TB) was added solid [Cu(MeCN)$_4$]PF_6 (1 mmol). The pale yellow solution was stirred for about 1 h at room temperature, concentrated under vacuum, and cooled in ice. The precipitate thus formed was collected by filtration and dried under vacuum.

[Cu(1-BB)]PF_6. Anal. Calcd for $C_{18}H_{19}N_5CuPF_6$: C, 42.07; H, 3.73; N, 13.63. Found: C, 42.15; H, 4.00; N, 13.45. IR (Nujol, cm^{-1}): 3355 m, 1618 m, 1499 s, 1487 s, 1400 w, 1330 w, 1296 w, 1263 w, 1247 w, 1228 w, 1087 m, 1009 w, 988 w, 942 w, 841 s, 775 w, 746 s.

[Cu(2-BB)]PF_6. Anal. Calcd for $C_{20}H_{23}N_5CuPF_6$: C, 44.33; H, 4.28; N, 12.92. Found: C, 44.05; H, 4.22; N, 12.62. IR (KBr, cm^{-1}): 3310 m, 3062 w, 1615 w, 1545 w, 1485 s, 1412 m, 1344 w, 1328 m, 1296 m, 1236 m, 1178 m, 1151 w, 1125 m, 1108 m, 1058 w, 1021 m, 1007 w, 975 w, 936 s, 835 vs, 748 s.

Table 10. Selected Positional Parameters and Their Estimated Standard Deviations for [Cu(2-BB)(NO$_2$)](ClO$_4$)(MeCN)

atom	*x*	*y*	*z*	$B_{eq}{}^a$ (Å^2)
Cu	0.9123(2)	0.6507(1)	0.74420(9)	3.29(3)
O5	0.620(1)	0.7286(7)	0.6484(5)	7.5(2)
O6	0.7048(9)	0.7677(5)	0.7661(4)	4.4(2)
N1	0.8434(9)	0.5225(5)	0.8573(5)	3.2(2)
N2	0.794(1)	0.3458(6)	0.9518(5)	3.8(2)
N3	1.0525(9)	0.7725(5)	0.6724(5)	3.4(2)
N4	1.2077(9)	0.8816(6)	0.5543(5)	3.7(2)
N5	1.026(1)	0.5423(5)	0.6755(5)	3.5(2)
N6	0.578(1)	0.7851(8)	0.7015(7)	6.3(3)
C1	0.849(1)	0.4134(7)	0.8607(6)	3.6(2)
C2	0.776(2)	0.2235(8)	0.9810(8)	6.0(3)
C3	0.753(1)	0.4142(7)	1.0062(5)	3.7(2)
C4	0.784(1)	0.5269(7)	0.9466(6)	3.3(2)
C5	0.690(1)	0.3895(8)	1.1026(6)	4.4(2)
C6	0.661(1)	0.4794(9)	1.1357(6)	4.8(3)
C7	0.694(1)	0.5929(8)	1.0781(6)	4.4(2)
C8	0.758(1)	0.6162(7)	0.9828(6)	3.7(2)
C9	1.145(1)	0.7812(7)	0.5922(6)	3.2(2)
C10	1.318(1)	0.9175(8)	0.4669(7)	4.8(3)
C11	1.152(1)	0.9467(1)	0.6133(6)	3.5(2)
C12	1.055(1)	0.8775(7)	0.6890(6)	3.4(2)
C13	1.175(1)	1.0553(8)	0.6080(7)	4.7(3)
C14	1.103(1)	1.0932(8)	0.6789(8)	5.4(3)
C15	1.008(1)	1.0245(8)	0.7574(8)	5.2(3)
C16	0.986(1)	0.9144(8)	0.7627(6)	4.3(2)
C17	0.898(1)	0.4590(7)	0.6828(7)	4.7(2)
C18	0.908(1)	0.3659(7)	0.7854(7)	4.4(2)
C19	1.046(1)	0.6108(8)	0.5660(6)	4.2(2)
C20	1.191(1)	0.6878(8)	0.5515(6)	4.5(2)

[a] $B_{eq} = (1/3)\sum_i \sum_j B_{ij} a_i{}^* a_j{}^* \mathbf{a}_i \cdot \mathbf{a}_j$.

[Cu(AcBB)]PF$_6$·H$_2$O. Anal. Calcd for $C_{22}H_{27}N_5O_2CuPF_6$: C, 43.89; H, 4.52; N, 11.63. Found: C, 44.02; H, 4.43; N, 11.43. IR (KBr, cm^{-1}): 3450 w, 3060 w, 2954 w, 1642 s, 1487s, 1415 m, 1338 w, 1245 s, 1158 w, 1011 m, 841 vs, 748 s.

[Cu(TB)]PF$_6$·H$_2$O. Anal. Calcd for $C_{31}H_{35}N_7CuO_3PF_6$: C, 48.85; H, 4.63; N, 12.86. Found: C, 48.83; H, 4.26; N, 12.65. IR (KBr, cm^{-1}): 3648 w, 3064 w, 1618 m, 1543 s, 1489 s, 1412 m, 1336 m, 1282 m, 1241 m, 1156 w, 1127 w, 1102 w, 1062 w, 1009 m, 839 vs, 746 s.

Copper(II) Complexes. The synthesis of these complexes was carried out according to the following general procedure. To a solution of the ligand in dichloromethane (2-BB, AcBB) or dichloromethane−ethanol (1-BB) was added the stoichiometric amount of copper(II) perchlorate hexahydrate dissolved in methanol. The product was precipitated by addition of diethyl ether, eventually after concentration of the solution under vacuum, and precipitation was completed by cooling in a refrigerator. The solid was filtered off, washed with small amounts of diethyl ether, and dried under vacuum.

[Cu(1-BB)][ClO$_4$]$_2$. Anal. Calcd for $C_{18}H_{19}N_5CuCl_2O_8$: C, 38.07; H, 3.37; N, 12.33. Found: C, 37.98; H, 3.92; N, 12.06. IR (Nujol, cm^{-1}): 3422 m, 3232 m, 1615 m, 1541 m, 1508 m, 1460 s, 1425 w, 1321 m, 1294 m, 1251 w, 1207 w, 1091 s, 1013 m, 946 m, 895 w, 770 s, 754 s, 721 w, 702 w, 625 s.

[Cu(2-BB)][ClO$_4$]$_2$. Anal. Calcd for $C_{20}H_{23}N_5CuCl_2O_8$: C, 40.31; H, 3.89; N, 11.75. Found: C, 40.78; H, 4.02; N, 11.78. IR (KBr, cm^{-1}): 3440 m, 3060 w, 2930 w, 1618 m, 1495 s, 1462 s, 1412 m, 1359 w, 1332 m, 1294 w, 1261 w, 1238 w, 1148 s, 1118 s, 1081 s, 1009 w, 973 w, 940 w, 862 w, 768 s, 627 s.

[Cu(AcBB)][ClO$_4$]$_2$·2MeOH. Anal. Calcd for $C_{24}H_{33}N_5CuCl_2O_{11}$: C, 41.06; H, 4.74; N, 9.98. Found: C, 41.15; H, 4.00; N, 10.04. IR (KBr, cm^{-1}): 3425 m, 3060 w, 2946 w, 1630 vs, 1485 m, 1435 s, 1340 w, 1296 w, 1245 w, 1216 w, 1189 w, 1154 w, 1010 br, 932 w, 880 w, 748 s, 638 s, 625 m.

The azide and nitrite adducts of the copper(II) complexes were obtained by adding a methanol solution of the sodium salt of the anion to an equimolar solution of the copper(II) complex in acetonitrile. When no spontaneous precipitation occurred even after cooling in a refrigerator, a small amount of diethyl ether was added to the cold solution, and precipitation was completed upon further cooling in the refrigerator. The product was then filtered off, washed with small amounts of cold water and diethyl ether, and dried under vacuum.

Table 11. Selected Bond Distances (Å) with Estimated Standard Deviations for [Cu(1-BB)(DMSO-*O*)$_2$](ClO$_4$)$_2$ (**IV**), [Cu(1-BB)(DMSO-*O*)$_2$](BF$_4$)$_2$](BF$_4$)$_2$ (**V**), and [Cu(1-BB)(DMSO-*O*)(NO$_2$)](ClO$_4$) (**VI**)

	IV	**V**	**VI**
Cu−O1	1.982(3)	1.980(4)	1.962(6)
Cu−O2	2.268(5)	2.242(6)	2.275(6)
Cu−O3			2.671(8)
Cu−N1	2.062(4)	2.040(5)	2.049(6)
Cu−N3	1.969(4)	1.967(5)	1.970(5)
Cu−N5	1.961(4)	1.958(6)	1.978(5)
N1−C1	1.469(6)	1.478(9)	1.45(1)
N1−C10	1.477(8)	1.47(1)	1.468(8)
N2−C2	1.355(6)	1.343(9)	1.348(8)
N2−C3	1.469(6)	1.477(8)	1.46(1)
N2−C4	1.376(7)	1.36(1)	1.388(9)
N3−C2	1.326(5)	1.321(8)	1.316(9)
N3−C5	1.391(7)	1.39(1)	1.396(8)
N4−C11	1.357(7)	1.35(1)	1.363(8)
N4−C12	1.453(8)	1.43(1)	1.44(1)
N4−C13	1.383(5)	1.368(8)	1.39(1)
N5−C11	1.317(6)	1.305(9)	1.306(9)
N5−C14	1.398(5)	1.401(8)	1.403(8)
C1−C2	1.483(8)	1.47(1)	1.494(9)
C4−C5	1.400(6)	1.414(8)	1.393(9)
C5−C9	1.388(8)	1.37(1)	1.40(1)
C5−C6	1.392(7)	1.38(1)	1.37(1)
C6−C7	1.391(9)	1.38(1)	1.40(1)
C7−C8	1.388(7)	1.40(1)	1.40(1)
C8−C9	1.381(8)	1.35(1)	1.35(1)
C10−C11	1.489(6)	1.501(9)	1.50(1)
C13−C14	1.391(8)	1.41(1)	1.39(1)
C13−C18	1.390(7)	1.41(1)	1.41(1)
C14−C15	1.387(7)	1.40(1)	1.35(1)
C15−C16	1.394(7)	1.39(1)	1.38(1)
C16−C17	1.41(1)	1.38(1)	1.38(1)
C17−C18	1.361(8)	1.36(1)	1.34(1)
S1−O1	1.536(4)	1.530(5)	
S1−C19	1.774(7)	1.767(9)	
S1−C20	1.772(6)	1.744(9)	
S2−O2	1.543(6)	1.570(8)	1.508(5)
S2−C21	1.73(1)	1.948(9)	1.76(1)
S2−C22	1.668(7)	1.51(2)	1.754(8)
S2′−O2	1.576(7)	1.563(9)	
S2′−C21	1.35(2)	1.66(1)	
S2′−C22	1.970(7)	1.75(1)	
O1−N6			1.25(1)
O3−N6			1.20(1)

[Cu(1-BB)(NO$_2$)]ClO$_4$. Anal. Calcd for $C_{18}H_{19}N_6CuClO_6$: C, 42.03; H, 3.72; N, 16.34. Found: C, 41.16; H, 3.21; N, 16.09. IR (KBr, cm^{-1}): 3616 m, 3532 m, 3208 m, 3068 w, 2960 m, 1620 m, 1597 m, 1526 s, 1499 s, 1485 s, 1458 s, 1425 s, 1390 m, 1321 m, 1294 m, 1272 w, 1249 w, 1098 s, 1011 m, 995 m, 942 m, 845 w, 775 m, 741 s, 700 w, 625 s.

[Cu(1-BB)(N$_3$)]ClO$_4$. Anal. Calcd for $C_{18}H_{19}N_8CuClO_4$: C, 42.36; H, 3.75; N, 21.95. Found: C, 41.99; H, 3.43; N, 21.42. IR (Nujol, cm^{-1}): 3628 w, 3410 w, 3096 w, 2110 s, 2060 w, 1615 w, 1506 m, 1458 s, 1350 w, 1319 w, 1294 w, 1251 w, 1094 s, 1011 m, 951 w, 938 w, 746 s, 623 s.

[Cu(2-BB)(NO$_2$)]ClO$_4$·MeOH. Anal. Calcd for $C_{21}H_{27}N_6CuClO_7$: C, 43.91; H, 4.74; N, 14.63. Found C, 43.69; H, 4.20; N, 14.31. IR (KBr, cm^{-1}): 3424 m, 3256 m, 2932 w, 2882 w, 1618 w, 1499s, 1462 s, 1417 m, 1334 m, 1307 w, 1294 w, 1257 w, 1238 w, 1183 m, 1100 s, 1015 m, 975 m, 934 w, 913 w, 861 w, 832 w, 768 s, 750 s, 625 s.

[Cu(2-BB)(N$_3$)]ClO$_4$·2MeOH. Anal. Calcd for $C_{22}H_{31}N_8CuClO_6$: C, 43.85; H, 5.19; N, 18.60. Found: C, 43.30; H, 4.88; N, 18.07. IR (KBr, cm^{-1}): 3370 w, 3224 m, 3060 w, 2922 w, 2054 s, 1613 w, 1495 m, 1483 w, 1458 m, 1415 m, 1332 w, 1294 w, 1259 w, 1241 w, 1191 w, 1098 s, 1011 w, 986 w, 930 w, 909 w, 864 w, 828 w, 768 s, 758 m, 623 m.

Table 12. Selected Bond Angles (deg) with Estimated Standard Deviations for [Cu(1-BB)(DMSO-*O*)$_2$](ClO$_4$)$_2$ (**IV**), [Cu(1-BB)(DMSO-*O*)$_2$](BF$_4$)$_2$ (**V**), and [Cu(1-BB)(DMSO-*O*)(NO$_2$)](ClO$_4$) (**VI**)

	IV	**V**	**VI**
O1−Cu−O2	101.6(2)	100.8(2)	90.9(2)
O1−Cu−O3			51.3(2)
O1−Cu−N1	169.5(2)	168.9(2)	173.9(3)
O1−Cu−N3	98.0(2)	98.3(2)	98.8(2)
O1−Cu−N5	96.9(1)	97.0(2)	99.3(2)
O2−Cu−N1	88.8(2)	90.3(2)	83.0(2)
O2−Cu−N3	91.5(2)	92.9(2)	99.5(2)
O2−Cu−N5	95.7(2)	95.2(2)	93.3(2)
O2−Cu−O3			141.3(2)
N1−Cu−N3	81.9(2)	82.0(2)	82.0(2)
N1−Cu−N5	81.5(2)	80.8(2)	81.3(2)
N1−Cu−O3			134.8(2)
N3−Cu−N5	161.8(2)	161.0(2)	157.6(2)
N3−Cu−O3			94.8(2)
N5−Cu−O3			86.5(2)
Cu−O1−S1	117.3(2)	117.9(3)	
Cu−O1−N6			112.1(5)
Cu−O2−S2	154.9(2)	122.7(4)	141.3(3)
Cu−O2−S2′	120.3(3)	151.1(3)	
Cu−O3−N6			78.1(5)
Cu−N1−C1	109.9(3)	109.4(5)	112.5(5)
Cu−N1−C10	111.0(3)	112.2(4)	113.1(4)
Cu−N3−C2	113.3(4)	114.3(5)	113.8(4)
Cu−N3−C5	139.5(3)	138.9(4)	140.8(4)
Cu−N5−C11	113.7(3)	114.7(4)	113.8(4)
Cu−N5−C14	139.6(4)	139.0(5)	140.6(5)
C1−N1−C10	115.4(4)	114.8(6)	114.2(6)
C2−N2−C3	125.9(5)	125.8(7)	127.9(6)
C2−N2−C4	107.2(3)	108.7(5)	106.4(6)
C3−N2−C4	126.7(4)	125.4(6)	125.7(5)
C2−N3−C5	105.7(4)	105.5(5)	105.4(5)
C11−N4−C12	126.5(4)	128.6(6)	128.0(6)
C11−N4−C13	106.7(4)	106.2(6)	104.8(5)
C12−N4−C13	126.8(5)	125.1(7)	127.2(6)
C11−N5−C14	106.6(4)	106.2(6)	105.6(5)
N1−C1−C2	106.1(4)	107.6(6)	107.0(6)
N2−C2−N3	112.3(5)	112.2(7)	113.3(6)
N2−C2−C1	127.7(4)	129.3(6)	125.6(6)
N3−C2−C1	120.0(4)	118.5(6)	121.0(6)
N2−4−C5	106.1(4)	104.8(6)	106.2(6)
N2−C4−C9	132.2(4)	132.9(5)	130.8(6)
C5−C4−C9	121.7(4)	122.2(7)	123.0(7)
N3−C5−C4	108.6(4)	108.7(6)	108.6(6)
N3−C5−C6	130.2(4)	131.5(5)	130.9(6)
C4−C5−C6	121.1(5)	119.7(7)	120.5(6)
C5−C6−C7	116.8(4)	117.8(6)	116.9(7)
C6−C7−C8	121.7(5)	121.2(7)	121.4(7)
C7−C8−C9	121.9(6)	121.7(8)	122.1(7)
C4−C9−C8	116.9(4)	117.4(6)	116.0(7)
N1−C10−C11	106.3(4)	105.7(6)	105.2(5)
N4−C11−N5	112.1(4)	113.6(5)	114.1(6)
N4−C11−C10	126.3(5)	125.9(7)	123.7(6)
N5−C11−C10	121.6(5)	120.5(7)	122.1(6)
N4−C13−C14	107.0(4)	107.4(6)	107.5(6)
N4−C13−C18	131.0(6)	132.5(8)	131.6(7)
C14−C13−C18	122.0(5)	120.0(7)	120.9(7)
N5−C14−C13	107.7(4)	106.7(6)	107.9(6)
N5−C14−C15	130.4(5)	131.5(8)	130.7(6)
C13−C14−C15	121.9(4)	121.8(6)	121.3(6)
C14−C15−C16	116.0(6)	115.9(8)	117.3(7)
C15−C16−C17	121.2(5)	122.5(7)	121.4(8)
C16−C17−C18	122.5(5)	121.8(7)	122.2(7)
C13−C18−C17	116.4(6)	117.9(9)	116.9(7)
O1−S1−C19	104.9(3)	104.4(4)	
O1−S1−C20	102.7(3)	103.3(4)	
C19−S1−C20	99.3(3)	99.3(4)	
O2−S2−C21	101.6(5)	97.8(5)	106.7(4)
O2−S2−C22	109.4(3)	113.1(7)	107.4(4)
C21−S2−C22	99.6(6)	100.3(6)	97.3(5)
O2−S2′−C21	119.8(7)	111.2(5)	
O2−S2′−C22	94.7(4)	101.4(6)	
C21−S2′−C22	101.0(5)	102.9(7)	
O1−N6−O3			118.5(8)

Table 13. Selected Bond Distances (Å) with Estimated Standard Deviations for [Cu(2-BB)(MeOH)(ClO$_4$)](ClO$_4$) (**I**), [Cu(2-BB)(N$_3$)](ClO$_4$) (**II**), and [Cu(2-BB)(NO$_2$)](ClO$_4$)(MeCN) (**III**)

	I	**II**	**III**
Cu−O1	2.333(7)		
Cu−O9	2.105(6)		
Cu−N1	1.954(7)	1.962(6)	1.965(6)
Cu−N3	1.958(7)	1.959(6)	1.964(7)
Cu−N5	2.021(8)	2.003(6)	2.017(7)
Cu−N6		1.946(6)	
Cu−O5			2.439(8)
Cu−O6			2.008(6)
Cl1−O1	1.453(7)		
Cl1−O2	1.409(7)		
Cl1−O3	1.403(9)		
Cl1−O4	1.392(9)		
O9−C21	1.42(1)		
N6−N7		1.150(8)	
N7−N8		1.172(9)	
O5−N6			1.23(1)
O6−N6			1.29(1)
N1−C1	1.30(1)	1.336(9)	1.34(1)
N1−C4	1.40(1)	1.38(1)	1.38(1)
N2−C1	1.35(1)	1.35(1)	1.38(1)
N2−C2	1.48(1)	1.48(1)	1.46(1)
N2−C3	1.36(1)	1.37(1)	1.36(1)
N3−C9	1.33(1)	1.32(1)	1.32(1)
N3−C12	1.39(1)	1.41(1)	1.42(1)
N4−C9	1.35(1)	1.36(1)	1.34(1)
N4−C10	1.47(1)	1.47(1)	1.47(1)
N4−C11	1.37(1)	1.39(1)	1.40(1)
N5−C17	1.45(1)	1.50(1)	1.51(1)
N5−C19a	1.40(2)	1.49(1)	1.53(1)
C5−C19b	1.33(2)		
C1−C18	1.51(1)	1.49(1)	1.45(1)
C3−C4	1.39(1)	1.42(1)	1.41(1)
C3−C5	1.38(1)	1.35(1)	1.41(1)
C4−C8	1.39(1)	1.39(1)	1.38(1)
C5−C6	1.39(2)	1.38(1)	1.36(2)
C6−C7	1.40(2)	1.42(1)	1.42(1)
C7−C8	1.37(1)	1.37(1)	1.40(1)
C9−C20	1.51(1)	1.48(1)	1.48(1)
C11−C12	1.40(1)	1.38(1)	1.40(1)
C11−C13	1.40(1)	1.41(1)	1.38(1)
C12−C16	1.37(1)	1.35(1)	1.37(1)
C13−C14	1.36(1)	1.35(1)	1.35(2)
C14−C15	1.39(2)	1.41(1)	1.42(1)
C15−C16	1.38(1)	1.40(1)	1.39(2)
C17−C18	1.49(2)	1.52(1)	1.52(1)
C19a−C20	1.41(2)	1.53(1)	1.54(2)
C19b−C20	1.53(2)		

[Cu(AcBB)(NO$_2$)]ClO$_4$·2MeOH. Anal. Calcd for $C_{24}H_{33}N_6CuClO_9$: C, 44.45; H, 5.13; N, 12.96. Found: C, 44.29; H, 4.70; N, 12.82. IR (KBr, cm^{-1}): 3422 m, 2958 w, 2816 w, 1630 s, 1485 s, 1425 s, 1377 m, 1360 w, 1296 w, 1245 w, 1216 w, 1154 m, 1081 w, 1011 s, 934 w, 841 w, 748 s 679 m.

[Cu(AcBB)(N$_3$)]ClO$_4$. Anal. Calcd for $C_{22}H_{25}N_8CuClO_5$: C, 45.52; H, 4.34; N, 19.30. Found: C, 45.22; H, 4.01; N, 19.15. IR (Nujol mull, cm^{-1}): 3080 sh, 2066 s, 1659 s, 1618 m, 1597 w, 1495 s, 1410 m, 1350 m, 1338 w, 1294 m, 1278 m, 1247 m, 1170 w, 1154 w, 1114 vs, 1062 s, 1025 w, 1002 w, 980 w, 932 w, 841 w, 754 s, 621 m.

[Cu(TB)(NO$_2$)]ClO$_4$·MeOH. Anal. Calcd for $C_{32}H_{37}N_8CuClO_9$: C, 49.49; H, 4.80; N, 14.43. Found: C, 49.00; H, 4.80; N, 14.18. IR (KBr, cm^{-1}): 3520 w, 3064 w, 2974 w, 1618 w, 1545 s, 1491 s, 1458 s, 1415 w, 1383 w, 1292 w, 1245 w, 1096 s, 1011 w, 932 w, 882 w, 845 w, 748 s, 623 s.

[Cu(TB)(N$_3$)]ClO$_4$·MeOH. Anal. Calcd for $C_{32}H_{37}N_{10}CuClO_7$: C, 49.74; H, 4.83; N, 18.13. Found: C, 49.40; H, 4.56; N, 18.00. IR (KBr, cm^{-1}): 3452 w, 3064 w, 2952 w, 2078 s, 2060 sh, 1618 w, 1543 s, 1493 s, 1458 s, 1412 w, 1338 w, 1290 w, 1241 w, 1098 s, 1011 w, 932 w, 882 w, 748 s, 623 s.

Small samples of the nitrite adducts were prepared similarly using Na^{15}NO$_2$.

Table 14. Selected Bond Angles (deg) with Estimated Standard Deviations for $[Cu(2\text{-}BB)(MeOH)(ClO_4)](ClO_4)$ (**I**), $[Cu(2\text{-}BB)(N_3)](ClO_4)$ (**II**), and $[Cu(2\text{-}BB)(NO_2)](ClO_4)(MeCN)$ (**III**)

	I	**II**	**III**
O1−Cu−O9	119.1(2)		
O1−Cu−N1	87.2(3)		
O1−Cu−N3	86.7(3)		
O1−Cu−N5	114.5(4)		
O9−Cu−N1	91.5(3)		
O9−Cu−N3	86.6(3)		
O9−Cu−N5	126.3(4)		
N1−Cu−N3	171.6(3)	150.5(3)	156.8(3)
N1−Cu−N5	94.5(3)	95.0(2)	93.4(3)
N3−Cu−N5	93.2(3)	91.1(3)	93.7(3)
N1−Cu−N6		94.0(3)	
N3−Cu−N6		98.5(3)	
N5−Cu−N6		142.5(3)	
O5−Cu−O6			55.5(3)
O5−Cu−N1			100.4(3)
O5−Cu−N3			100.6(3)
O5−Cu−N5			97.2(3)
O6−Cu−N1			91.0(3)
O6−Cu−N3			92.8(3)
O6−Cu−N5			152.6(3)
Cu−O1−Cl1	120.1(3)		
Cu−O9−C21	131.2(6)		
Cu−N1−C1	124.2(6)	125.7(6)	124.8(6)
Cu−N1−C4	128.5(5)	127.5(4)	127.3(6)
Cu−N3−C9	126.6(5)	125.7(5)	127.2(7)
Cu−N3−C12	125.6(5)	125.8(5)	126.6(6)
Cu−N5−C17	117.3(7)	111.7(5)	108.2(5)
Cu−N5−C19a	119.2(9)	106.2(4)	111.3(5)
Cu−N5−C19b	122(1)		
Cu−N6−N7		124.6(4)	
Cu−O5−N6			105.1(6)
Cu−O5−N6			85.9(6)
O1−Cl1−O2	107.8(5)		
O1−Cl1−O3	108.0(4)		
O1−Cl1−O4	109.7(4)		
O2−Cl1−O3	110.4(5)		
O2−Cl1−O4	111.2(5)		
O3−Cl1−O4	109.7(6)		
N6−N7−N8		176.3(9)	
O5−N6−O6			113.5(8)
C1−N1−C4	106.5(7)	106.8(6)	107.9(6)
C1−N2−C2	126.6(7)	127.3(7)	124.9(8)
C1−N2−C3	108.0(7)	109.0(6)	108.5(7)
C2−N2−C3	125.4(8)	123.7(7)	126.6(8)
C9−N3−C12	106.8(7)	108.1(6)	105.7(7)
C9−N4−C10	127.4(7)	126.1(6)	126.5(8)
C9−N4−C11	107.9(7)	107.5(6)	108.1(7)
C10−N4−C11	124.6(8)	126.3(7)	125.4(8)
C17−N5−C19a	119(1)	111.1(6)	107.0(7)
C17−N5−C19b	118.(1)		
N1−C1−N2	111.7(7)	110.7(7)	109.3(8)
N1−C1−C18	123.8(8)	125.2(7)	128.0(7)
N2−C1−C18	124.4(8)	124.1(6)	122.7(8)
N2−C3−C4	106.0(7)	104.9(7)	106.6(7)
N2−C3−C5	132.0(9)	131.6(7)	131.6(8)
C4−C3−C5	121.9(8)	123.4(7)	121.8(9)
N1−C4−C3	107.8(7)	108.6(6)	107.7(8)
N1−C4−C8	131.5(8)	132.5(7)	132.0(7)
C3−C4−C8	120.8(8)	118.8(7)	120.3(8)
C3−C5−C6	116.8(9)	117.6(7)	116.8(8)
C5−C6−C7	121.4(9)	120.1(9)	122.6(9)
C6−C7−C8	121.2(9)	121.4(8)	120(1)
C4−C8−C7	117.9(9)	118.5(7)	118.4(8)
N3−C9−N4	111.3(7)	110.6(6)	112.8(8)
N3−C9−C20	125.9(8)	127.4(7)	124.8(7)
N4−C9−C20	122.8(8)	122.0(7)	122.2(8)
N4−C11−C12	106.3(7)	107.3(7)	105.6(8)
N4−C11−C13	131.4(8)	132.0(8)	132.8(8)
C12−C11−C13	122.4(7)	120.7(7)	121.5(9)
N3−C12−C11	107.7(7)	106.5(7)	107.8(8)
N3−C12−C16	131.5(8)	130.9(8)	131.4(8)
C11−C12−C16	120.8(8)	122.6(7)	120.8(9)
C11−C13−C14	115.7(9)	116.7(8)	117.9(9)
C13−C14−C15	121.8(9)	122.9(8)	122.(1)
C14−C15−C16	122.8(8)	119.3(8)	120.(1)
C12−C16−C15	116.6(9)	117.8(8)	117.7(8)
N5−C17−C18	114.6(3)	110.5(7)	111.2(8)
C1−C18−C17	112.3(9)	113.6(6)	113.6(7)
N5−C19a−C20	125.(1)	111.1(7)	110.5(7)
N5−C19b−C20	121.(2)		
C9−C20−C19a	114.(1)	113.8(7)	115.1(8)
C9−C20−C19b	119(1)		

Caution! Although we did not have problems working with small amounts of the perchlorate complexes reported in this study, extreme care should be exercised in handling materials containing this shock-sensitive anion.

Nitrite Reductase Activity. The reactions between $[Cu(1\text{-}BB)]^+$, $[Cu(2\text{-}BB)]^+$, $[Cu(AcBB)]^+$, $[Cu(TB)]^+$, and nitrite were performed at room temperature as follows. To a degassed solution of Cu(I) complex (2.7×10^{-5} mol) in dry MeCN (1 mL) were added a few microliters of degassed solutions of $NaNO_2$ (2.7×10^{-5} mol) in methanol and $HBF_4 \cdot Et_2O$ (5.4×10^{-5} mol) in diethyl ether. A weak argon stream bubbled through the solution delivered the gas evolved from the reaction into a degassed 1×10^{-2} M Fe(EDTA) solution in 1 M aqueous citrate buffer, pH 5.0, which was kept cooled in an ice bath. After interruption of the argon flow, the amount of NO evolved in the reaction was estimated from the intensity of the characteristic absorption of the [Fe(EDTA)(NO)] complex at 432 nm ($\epsilon = 590$ M^{-1} cm^{-1}). The reactions between the Cu(I) complexes and $(NO^+)(BF_4^-)$ were performed similarly. The extinction coefficient used for the [Fe(EDTA)(NO)] complex refers to the operation conditions of the experiments and was determined by bubbling NO gas through the degassed 0.01 M Fe(EDTA) solution for 5 min and reading its absorbance at 432 nm. Blank determinations of NO recovery from reduction of nitrite by ascorbate under the gas flow conditions used in the reactions were carried out on methanol−acetonitrile (1:1, v/v) solutions containing $NaNO_2$ (0.01 M) and yielded an average of 83% NO (as [Fe(EDTA)(NO)] complex) after 5 min. The yields of NO reported in Table 3 are relative yields calculated on the basis of the effective recovery of NO in the blank experiments. The experiments were run in duplicate with high reproducibility (differences were less than 5%).

Structure Determinations. Crystals of $[Cu(1\text{-}BB)(DMSO\text{-}O)_2](ClO_4)_2$ and $[Cu(1\text{-}BB)(NO_2)(DMSO\text{-}O)](ClO_4)$ were obtained by dissolution of the complex in DMSO followed by addition of an equal volume of diethyl ether and a half-volume of THF. Crystals of $[Cu(2\text{-}BB)(MeOH)(ClO_4)](ClO_4)$ were obtained upon slow evaporation of a methanolic solution of the complex. Crystals of $[Cu(2\text{-}BB)(N_3)](ClO_4)$ and $[Cu(2\text{-}BB)(NO_2)](ClO_4)$ were grown by diffusion of diethyl ether in a MeCN solution of the complex. Crystals of $[Cu(1\text{-}BB)(DMSO\text{-}O)_2](BF_4)_2$ from the reaction of $[Cu(1\text{-}BB)]PF_6$ with nitrite were obtained as follows. The Cu(I) complex (13.9 mg, 0.027 mmol) dissolved in MeCN (2 mL) was reacted with a 0.03 M methanol solution of $NaNO_2$ (0.027 mmol) and a 7.45 M diethyl ether solution of HBF_4 (0.054 mmol) under a stream of argon. The reaction was continued for about 1 h, after which the product $[Cu(1\text{-}BB)](BF_4)(PF_6)$ was precipitated by addition of diisopropyl ether {IR (cm^{-1}): 1080 vs, br, $\nu(BF_4)$; 839 s, $\nu(PF_6)$. UV−vis and EPR spectra were identical with those of $[Cu(1\text{-}BB)]^{2+}$}. Crystallization from a mixture of DMSO−diethyl ether−THF as described above deposited crystals of $[Cu(1\text{-}BB)(DMSO\text{-}O)_2](BF_4)_2$.

Data were collected on an Enraf-Nonius CAD-4 diffractometer with graphite-monochromated Cu Kα radiation ($\lambda = 1.541\ 84$ Å) at 293(2) K in the 2−70° θ range. Calculations were performed on a MicroVax 3100 computer with SDP and MolEN software.[42,43] Crystal data and pertinent experimental details are given in Table 4. Atomic scattering

---

(42) *SDP Structure Determination Package*; B. A. Frenz and Associates and Enraf-Nonius: College Station, TX, and Delft, The Netherlands, 1990.

(43) *MolEN: An Interactive Structure Solution Procedure*; Enraf-Nonius: Delft, The Netherlands, 1990.

factors, with anomalous dispersion corrections, were taken from ref 44. All the structures were solved by direct methods (MULTAN80).[45] Besides the exceptions listed below, in all the structures the non-hydrogen atoms were anisotropically refined by full-matrix least squares, while the hydrogen atoms were not refined. The positions of the nonacidic hydrogen atoms were calculated, with the exception of those of $[Cu(2\text{-BB})(N_3)](ClO_4)$, where they were experimentally found.

In $[Cu(2\text{-BB})(MeOH)(ClO_4)](ClO_4)$, one of the carbon atoms (C19) was found statistically disordered between two slightly different positions (multiplicity of each position = 0.5). The hydrogen atoms bonded to N5, C19, and C20 were disregarded. In $[Cu(2\text{-BB})(N_3)](ClO_4)$, the hydrogen atom of the amine N−H group was isotropically refined. In $[Cu(2\text{-BB})(NO_2)](ClO_4)$, a disordered MeCN solvation molecule is present, which was refined isotropically; in the final ΔF map positive and negative residuals were found near this molecule. Permutation of the labels of the C and N terminal atoms of this MeCN molecule produced inconsistent results. Also the perchlorate anion seems quite disordered, because of the high thermal parameters of its oxygen atoms. In both $[Cu(1\text{-BB})(DMSO\text{-}O)_2](ClO_4)_2$ and $[Cu(1\text{-BB})(DMSO\text{-}O)_2](BF_4)_2$, the dimethyl sulfoxide ligand in the apical position is disordered, with the sulfur atom statistically distributed on opposite sides of the plane defined by the atoms O2, C21, and C22; moreover, in both structures the counterion farthest from the complex (the perchlorate of Cl2 and the tetrafluoroborate of B2) seems quite disordered; in the final ΔF maps postive and negative residuals are found near these molecules. Selected positional parameters are given in Tables 5−10. Selected bond distances and angles are reported in Tables 11−14. Further details are presented in the Supporting Information.

Acknowledgment. This work was supported by the European Community, allowing regular exchange of preliminary results with several European colleagues, under Contract ERBCHRXCT920014, and by the Italian MURST.

Supporting Information Available: A view of the $[Cu(1\text{-BB})(DMSO\text{-}O)_2]^+$ cation in the $[Cu(1\text{-BB})(DMSO\text{-}O)_2](BF_4)_2$ crystal and tables of complete atomic coordinates, anisotropic thermal parameters, bond lengths and angles, and the details of the crystallographic analyses of the copper(II) structures (44 pages). Ordering information is given on any current masthead page.

IC950392O

---

(44) *International Tables for X-ray Crystallography*; Kynoch: Birmingham, U.K., 1974; Vol. IV.

(45) Main, P.; Hull, S. E.; Lessinger, L.; Germain, G.; Declerq, J. P.; Woolfson, M. M. *MULTAN80: A System of Computer Programs for the Automatic Solution of Crystal Structures from X-ray Diffration Data*; Universities of York and Louvain: York, England, and Louvain, Belgium, 1980.